Response to Editor

Dear authors,

thank you very much for the revised version of your manuscript. Since all other reviewers suggested minor revisions, I only requested one of the reviewers (René Orth) to comment on the new version.

He appreciates the additional analyses performed, but still feels that some of the variables have not been validated, such as run-off. The reviewer suggests additional analyses, regarding (1) use updated version of the Jung et al. dataset (Jung et al., 2019) and (2) use the E-RUN dataset (Gudmundsson and Seneviratne, 2016) to validate the runoff.

I find that the manuscript has much improved and you have made good effort addressing the reviewers comments. I think the manuscript is almost ready for publication, given some amendments. In view of the fact that the Jung et al. (2019) paper was published only after the submission of the manuscript (although the data were available earlier), I will not insist on this additional analysis. However, please consider the Gudmundson and Seneviratne (2016) dataset. Please also attend to the detailed comments of the reviewer.

I am looking forward to your resubmitted manuscript,

Anke Hildebrandt.

Response: We thank the editor for the evaluation and comment on the revised manuscript. As suggested by the editor and reviewer, we have conducted additional analyses using the E-RUN database (Gudmundson and Seneviratne, 2016) and the FLUXCOM database (updated version of MPI database, Jung et al., 2019). We also revised the manuscript accordingly as well as conducted a point-by-point response to all the comments by the reviewer.

The main comment here is a further cross-validation of the CDR runoff based on the E-RUN database. The comparison results show that both the long-term mean ($\bar{Q}$) and standard deviation (σ_Q) of the monthly runoff in the E-RUN database are very similar with those in the CDR database. We further added the comparison results of runoff in the revised Supplementary Material, and also changed the text accordingly in the revised manuscript. Please also see R2C3 for a detailed response to this point.

Another comment is about using the FLUXCOM database instead of MPI in the validation of the CDR evapotranspiration E. As has been noted by the editor, the FLUXCOM database paper was published after the submission of this manuscript. In addition, the monthly FLUXCOM data is currently only available (open to public) for a much shorter period (2001-2010) compared with both the monthly CDR (1984-1010) and the original MPI (1982-1011) databases. As strongly suggested by R2, we conducted further comparison between the CDR and FLUXCOM databases, and the results are similar with those comparison between the CDR and MPI databases. Given the limited time period in the FLUXCOM database and the similarity of comparison results using the MPI and FLUXCOM databases, we choose to keep the results of the MPI database in the Supplementary Material. Please also see R2C2 for detailed response.

Again, we sincerely appreciate both the editor and reviewer for constructive suggestions and comments on the revised manuscript.

Response to Referee #2 (Dr René Orth)

R2C1: Second review of Yin and Roderick "Inter-annual variability of the global terrestrial cycle"

The paper has overall improved as the authors have addressed many of the concerns raised by me and the other reviewers. However, one important issue, and several minor points remain unresolved.

Response: We thank Dr René Orth for the evaluation and helpful comments on the revised manuscript. Please see detailed response to all the comments as follows.

R2C2: Main comment: As mentioned in my previous review, I think it is critical for this study to show that the discovered patterns are not just implemented in the model used to derive the CDR dataset. It has to be shown that similar patterns are present across independent datasets, as only this can indicate that nature is indeed operating this way. I appreciate efforts in this direction made by the authors, namely the consideration of the LandFlux-EVAL dataset, the Jung et al. dataset, and the ERA5 reanalysis. But I believe that these analyses need to be expanded before the paper can be published:

(1) I understand that the authors do not want to use GLEAM as a reference dataset as this was used in the derivation of the CDR reanalysis. But instead the Jung et al. dataset should be updated to the 2019 version (Jung et al. 2019). The authors stated in their response: 'We could replace the MPI we used with the updated database (Jung et al., 2019) but we do not see how that would alter the results.' This is not about altering the results, but about using state-of-the-art alternative datasets to illustrate the robustness of the CDR-based results. I do not see the point in using an almost 10-year old dataset while updated and much evolved datasets exist.

Response: As suggested by R2, we conducted further comparison between the CDR and FLUXCOM (0.5° × 0.5°, monthly, 2001-2010) (updated version of MPI database, Jung et al., 2019) databases, and the results are shown in Fig. R1. The results are similar with the previous comparison between the CDR and MPI databases, showing underestimation of the monthly mean E and bias and scaling offset in the standard deviations of monthly E in the CDR database compared with the FLUXCOM database.

However, currently the monthly FLUXCOM database is only available (open to public) for the restricted period 2001-2010, which is much shorter than both the CDR (available during 1984-2010) and the MPI (available during 1982-2011) databases. Given the limited time period for the FLUXCOM database and the similar comparison results of the MPI and FLUXCOM to the CDR databases, we propose to keep the results based on the original MPI database in the Supplementary material.

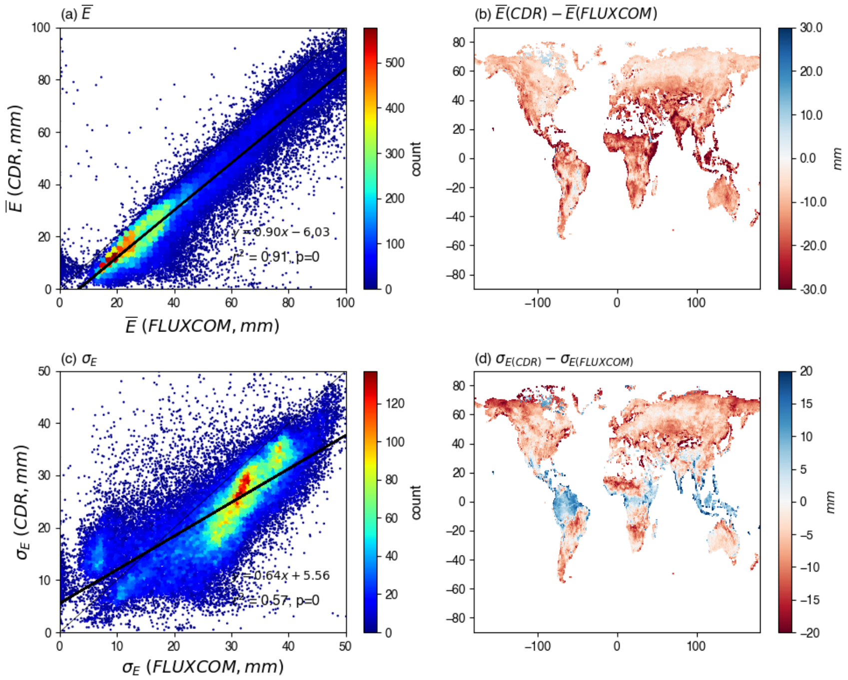

Figure R1. Comparison of monthly evapotranspiration *E* between FLUXCOM and Climate Data Record (CDR) databases. Top panels (a) (b) show comparison of the mean monthly ($\overline{E}$) while bottom panels (c) (d) show comparison of the standard deviation (σ_E) of monthly *E*.

R2C3: (2) I also appreciate the ERA5-based analyses which the authors have done in response to my previous comments. I share their conclusion that this dataset is not suitable to be used in the context of this study. However, this way the runoff results remain not confirmed with independent data. Therefore I suggest to use the E-RUN gridded runoff dataset (Gudmundsson and Seneviratne 2016) for this purpose.

I do not wish to remain anonymous - Rene Orth.

Response: As suggested, we conduct further comparison of the monthly runoff between the E-RUN (0.5° × 0.5°, monthly, 1951-2015) (Gudmundsson and Seneviratne, 2016) and CDR databases. The comparison is conducted based on the overlap of time (1984-2010) and space (Europe) in both databases, and the results are shown in Figs. R2-R3. We can see that both the long-term mean ($\overline{Q}$) and standard deviation (σ_Q) of the monthly runoff show very similar spatial patterns in the E-RUN and CDR databases (Fig. R2). The grid-by-grid comparison also shows close agreement (Fig. R3). We have added these results to the revised Supplementary Material (Figs. S10-S11), and also added the text in the revised manuscript as follows (lines 165-169): "*The comparison of runoff Q between the E-RUN and CDR databases show that the two databases have very similar spatial patterns of both the long-term mean ($\overline{Q}$) and standard deviation (σ_Q) of the monthly Q (Fig. S10). The grid-by-grid comparison results are also encouraging, showing slight bias of both the long-term mean and standard deviation of monthly Q in the CDR database compared with the E-RUN database (Fig. S11).*".

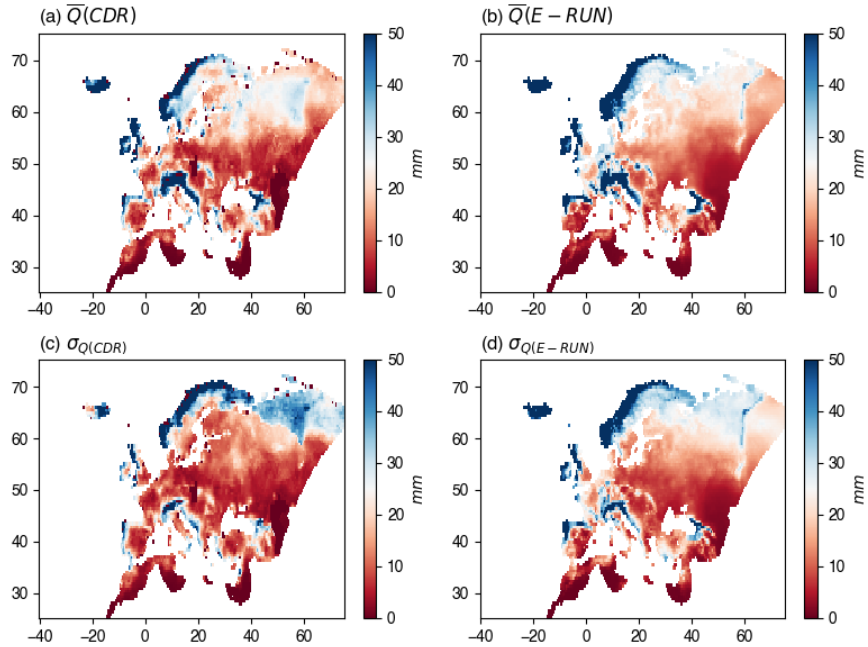

Figure R2. Mean ($\overline{Q}$) and standard deviation (σ_Q) of monthly runoff Q in the E-RUN and Climate Data Record (CDR) databases in the area of spatial overlap (Europe). Top panels (a) (b) show the mean monthly ($\overline{Q}$) while bottom panels (c) (d) show the standard deviation (σ_Q) of monthly Q.

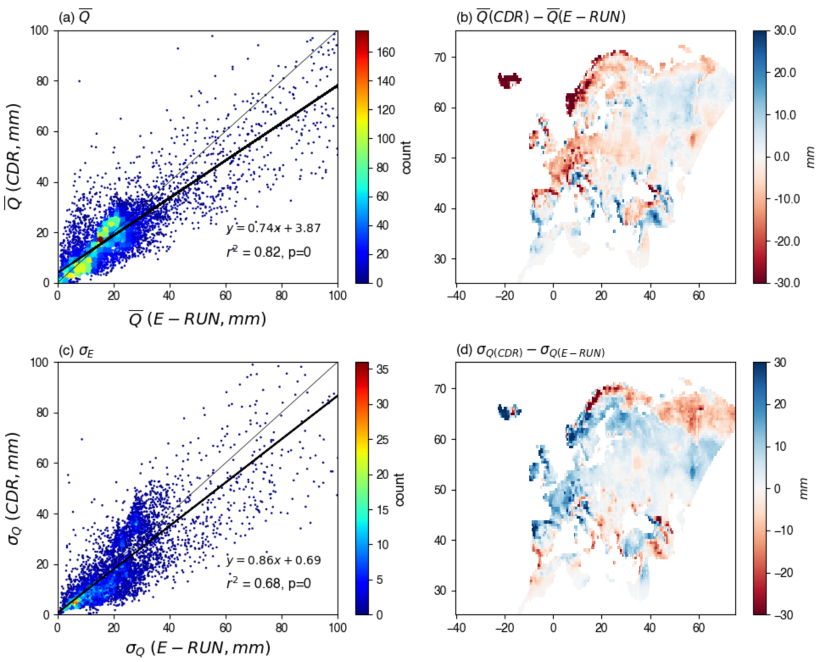

Figure R3. Comparison of monthly runoff Q between the E-RUN and Climate Data Record (CDR) databases in the area of spatial overlap (Europe). Top panels (a) (b) show comparison of the mean monthly ($\overline{Q}$) while bottom panels (c) (d) show comparison of the standard deviation (σ_Q) of monthly Q.

Specific comments:

R2C4: lines 53-55: This statement somewhat ignores the efforts leading to the ERA-Land (Balsamo et al. 2013) and MERRA-Land (Reichle et al. 2011) datasets.

Response: We have acknowledged the efforts in developing land-based products in the revised manuscript by modifying the sentence to (lines 53-57): "*Though efforts have been taken to develop land-based products from atmospheric reanalyses, e.g., ERA-Land (Balsamo et al. 2013) and MERRA-Land (Reichle et al. 2011) databases, however, the central aim of atmospheric re-analysis is to estimate atmospheric variables. That atmospheric-centric aim, understandably, ignores many of the nuances of soil water infiltration, vegetation water uptake, runoff generation and many other processes of central importance in hydrology.*". The relevant reference has also been cited in the revised manuscript.

R2C5: line 75: 'the various ... databases' - after only reading the text up to this point it is not clear what is meant here

Response: It means the databases used in this study will be introduced and described in Section 2. To make this sentence more clear, we have modified it in the revised manuscript as follows (lines 77-79): "*We begin in Section 2 by describing the various climate and hydrologic databases used in this study, and also include a further assessment of the suitability of the CDR database for this initial variability study.*".

R2C6: line 78: it should be 'these variabilities'

Response: Done. Thank you.

R2C7: lines 88/89: 'in time step t' - these are all fluxes which are accumulated during time steps t-1 and t; also, I would mention here that the time step considered in this study is 1 year

Response: We have added the annual time step in this sentence to make it more clear in the revised version (lines 90-91): "*with P the precipitation, E the evapotranspiration, Q the runoff and ΔS the total water storage change in time step t (annual in this study).*". Thank you.

R2C8: lines 91/92: 'Eq (1) is the familiar...' - this sentence is an unnecessary repetition

Response: This sentence has been deleted in the revised manuscript. Thanks.

R2C9: line 96: known here?

Response: To make the meaning of this sentence more clear, we have removed the word 'known' and modified it in the revised manuscript as follows (lines 98-99): "*We use the Climate Data Record (CDR) database (Zhang et al., 2018) which is a recently released global land hydrologic re-analysis.*".

R2C10: line 103: The SRB dataset only extents until 2007 (if I am not mistaken) while the analyses in this study consider a time period until 2010. How can you still use the SRB data then?

Response: The aim of this study is to investigate the inter-annual variability of global water cycle based on the CDR database, which extends from 1984 to 2010. During the construction process, the CDR database made some assumptions considering the 27-year period (1984-2010) as an integrity, e.g., the long-term (27-year) storage change to be zero. To better investigate the inter-annual variability by using the CDR database in this study, we choose to stick to the CDR period, i.e., 1984-2010.

While the SRB database is only available from 1984 to 2007 (not to 2010), we only use it to calculate the long-term E_0 ($\overline{E_o}$) and further estimate the aridity index ($\overline{E_o}/\bar{P}$). We believe the three-year period difference would not have a material impact on the aridity index estimation or change the general conclusions in this study. Thanks.

R2C11: lines 105/106: Sentence is hard to understand, please rephrase.

Response: We have rephrased this sentence in the revised manuscript as follows (lines 107-108): "*In general, we anticipate two important factors, i.e., the water storage capacity and the presence of ice/snow at the surface, which are most likely to have influence on the partitioning of hydrologic variability.*". Thanks.

R2C12: line 160: Please comment on the offset.

Response: We have added more details for the offset and modified the sentence in the revised manuscript as follows: "*In terms of variability, the standard deviations of monthly E from the CDR are in very close agreement with the LandFluxEVAL database (Fig. S7c), but there is a bias and scaling offset for the comparison with the MPI database particularly for the grid-cells with low standard deviation of E (Fig. S8c).*".

R2C13: line 177: I would replace 'trend' with 'pattern'

Response: Done. Thank you.

R2C14: line 180: not clear what is meant here with 'physics of runoff generation'

Response: Yes, we agree that the 'physics of runoff generation' is not clear and we have replaced it with more specific term in the revised manuscript as follows (lines 187-189): "*However, there is substantial scatter due to, for example, regional variations related to seasonality, water storage change and the landscape characteristics*".

R2C15: lines 178-181: Padron et al. 2017 is relevant in this context, and could be cited.

Response: The reference has now been cited in the revised manuscript. Thank you.

R2C16: lines 188, 203, 223: 'very different' is not obvious to me from the comparison of Figs 1 and 3. Please clarify.

Response: Here we mean it is very different between the partitioning of $\bar{P}$ and σ_P^2. In brief, the $\bar{P}$ is mostly partitioned into $\bar{E}$ or $\bar{Q}$. However, for the partitioning of σ_P^2, σ_E^2 is generally very small with σ_P^2 mostly partitioned into σ_Q^2, $\sigma_{\Delta S}^2$ and even the covariance components. Please see the more comprehensive and detailed analyses in the revised manuscript (lines 199-209).

R2C17: lines 225-226: This is an important finding which should be highlighted in the abstract and/or conclusions.

Response: Yes, the finding here has been added in the abstract (lines 11-12): "*Instead we find that σ_P^2 is mostly partitioned between σ_Q^2, $\sigma_{\Delta S}^2$ and the associated covariances with limited partitioning to σ_E^2.*".

R2C18: lines 294-303: If the main conclusion is that things are complex, and there is no particular lesson learned here, then I would suggest to remove this section. It confuses readers and distracts from the relevant main messages of the study.

Response: While the results here are complex and not easy to understand, we still could have some implications obtained here, for example, the difference between partitioning of σ_P^2 at high and low temperature. That difference does show the important role of temperature in the partitioning of σ_P^2, which might be helpful for the future studies. Therefore, we would like to keep this section in the revised manuscript.

R2C19: lines 307-328: It feels inconsistent that in addition to the wet and hot grid cell no wet and cold grid cell has been selected as a case study (as was done in the case of high and low water storage capacity).

Response: The reason we did not pick any case study site here is because there is substantial scatter in wet and cold conditions ($\overline{E_o}/\bar{P} \leq 0.5$ in first column of Fig. 8). The partitioning of σ_P^2 in wet and cold conditions is so complex that no grid-cell could be chosen as a representative case study site. Instead of a case study site, we further illustrate the importance of snow/ice presence in variance partitioning (lines 425-426) and expect more emphasis on this in the future studies that our manuscript will inspire.

R2C20: - While this study is performed at annual time scales, the authors could add some outlook/clarification that the revealed variability propagation across the water cycle might behave differently at shorter time scales

Response: Yes, we agree that the variability partitioning might be different at various time scales. In response, we have added an expectation for future work at various time scales in the revised manuscript (lines 408-410): "*These general principles of variance partitioning in the water cycle above may vary at different time scales (e.g., monthly, daily), and we expect more details of the variability partitioning across various temporal scales to be investigated in future studies.*".

R2C21: - Figures 2,5, and others display physically implausible values - please comment on this

Response: Yes, there are some grid-cells showing physically implausible values in Figs. 2 and 5. In this study, we have tried to exclude the grid-cells with high uncertainty (please see Section 2.3 and Fig. S2), therefore, it is unlikely that those implausible values are caused by data uncertainty/error. While checking the location of those grid-cells, we found that they almost appear in/close to the Greenland. Therefore, we guess those physically implausible values are caused by the permanent ice/glacier. As also noted in this study, with the presence of snow/ice, it is very complex in the variance partitioning. In this study, we highlighted regions with snow/ice coverage. We except future studies to further uncover the role of snow/ice in the variance partitioning and show details of these physically implausible values.

R2C22: - It is not intuitive that non-consistent (logarithmic/non-lagarithmic) axes are used for E0/P across different figures.

Response: Yes, the axes for the aridity index (E_o/P) are linear in Figs. 2, 5 and 6 and logarithmic in Figs. 7 and 8. The underlying reason for that is because there are different purposes in presenting the results in these figures. In Figs. 2, 5 and 6, we show the relation of long-term mean and variance to E_o/P. It is better to use the regular non-logarithmic axes to compare with results in previous studies (e.g., Budyko-curve and Koster and Suarez analyses) that also use linear axes. While in Figs. 7 and 8, we highlight the role of storage capacity and physical phase (solid/liquid) in variance partitioning in both extremely dry and wet environments. We found the logarithmic axes to better show the necessary details in Figs. 7 and 8.

R2C23: References:

Balsamo, G., C. Albergel, A. Beljaars, S. Boussetta, E. Brun, H. Cloke, D. Dee, E. Dutra, J. Muñoz-Sabater, F. Pappenberger, P. de Rosnay, T. Stockdale, and F. Vitart, 2013: ERA Interim Land: a global land water resources dataset. Hydrol. Earth Syst. Sci., 19, 389–407.

Gudmundsson, L., and S.I. Seneviratne, 2016: Observation-based gridded runoff estimates for Europe (E-RUN version 1.1). Earth Syst. Sci. Data, 8 (2), 279–295.

Jung, M., S. Koirala, U. Weber, K. Ichii, F. Gans, G. Camps-Valls, D. Papale, C. Schwalm, G. Tramontana, and M. Reichstein, 2019: The FLUXCOM ensemble of global land-atmosphere energy fluxes. Scientific Data, 6 (74).

Padron, R.S., L. Gudmundsson, P. Greve, and S.I. Seneviratne, 2017: Large- Scale Controls of the Surface Water Balance Over Land: Insights From a Systematic Review and Meta-Analysis. Water Res. Resour., 53 (11), 9659-9678.

Reichle, R.H., R.D. Koster, G.J.M.D. Lannoy, B.A. Forman, Q. Liu, S.P.P. Mahanama, and A. Toure, 2011: Assessment and enhancement of MERRA land surface hydrology estimates. J. Clim., 24, 6322–6338,

Response: We thank Dr René Orth for listing all the reference in the comments, and we have read and cite these reference accordingly in the revised manuscript.

Inter-annual variability of the global terrestrial water cycle

Dongqin Yin[1,2], Michael L. Roderick[1,3]

[1]Research School of Earth Sciences, Australian National University, Canberra, ACT, 2601, Australia

[2]Australian Research Council Centre of Excellence for Climate System Science, Canberra, ACT, 2601, Australia

[3]Australian Research Council Centre of Excellence for Climate Extremes, Canberra, ACT, 2601, Australia

Correspondence to: (dongqin.yin@anu.edu.au)

Abstract:

Variability of the terrestrial water cycle, i.e., precipitation (*P*), evapotranspiration (*E*), runoff (*Q*) and water storage change (ΔS) is the key to understanding hydro-climate extremes. However, a comprehensive global assessment for the partitioning of variability in *P* between *E*, *Q* and ΔS is still not available. In this study, we use the recently released global monthly hydrologic reanalysis product known as the Climate Data Record (CDR) to conduct an initial investigation of the inter-annual variability of the global terrestrial water cycle. We first examine global patterns in partitioning the long-term mean $\bar{P}$ between the various sinks $\bar{E}$, $\bar{Q}$ and $\overline{\Delta S}$ and confirm the well-known patterns with $\bar{P}$ partitioned between $\bar{E}$ and $\bar{Q}$ according to the aridity index. In a new analysis based on the concept of variability source and sinks we then examine how variability in the precipitation σ_P^2 (the source) is partitioned between the three variability sinks σ_E^2, σ_Q^2 and $\sigma_{\Delta S}^2$ along with the three relevant covariance terms, and how that partitioning varies with the aridity index. We find that the partitioning of inter-annual variability does not simply follow the mean state partitioning. Instead we find that σ_P^2 is mostly partitioned between σ_Q^2, $\sigma_{\Delta S}^2$ and the associated covariances with limited partitioning to σ_E^2. We also find that the magnitude of the covariance components can be large and often negative, indicating that variability in the sinks (e.g., σ_Q^2, $\sigma_{\Delta S}^2$) can, and regularly does, exceed variability in the source (σ_P^2). Further investigations under extreme conditions revealed that in extremely dry environments the variance partitioning is closely related to the water storage capacity. With limited storage capacity the partitioning of σ_P^2 is mostly to σ_E^2, but as the storage capacity increases the partitioning of σ_P^2 is increasingly shared between σ_E^2, $\sigma_{\Delta S}^2$ and the covariance between those variables. In other environments (i.e., extremely wet and semi-arid/semi-humid) the variance partitioning proved to be extremely complex and a synthesis has not been developed. We anticipate that a major scientific effort will be needed to develop a synthesis of hydrologic variability.

Deleted:

1. Introduction

In describing the terrestrial branch of the water cycle, the precipitation (P) is partitioned into evapotranspiration (E), runoff (Q) and change in water storage (ΔS). With averages taken over many years, $\overline{\Delta S}$ is usually assumed to be zero and it has long been recognized that the partitioning of the long-term mean annual precipitation ($\bar{P}$) between $\bar{E}$ and $\bar{Q}$ was jointly determined by the availability of both water ($\bar{P}$) and energy (represented by the net radiation expressed as an equivalent depth of water and denoted $\overline{E_o}$). Using data from a large number of watersheds, Budyko (1974) developed an empirical relation relating the evapotranspiration ratio ($\bar{E}/\bar{P}$) to the aridity index ($\overline{E_o}/\bar{P}$). The resultant empirical relation and other Budyko-type forms (e.g., Fu, 1981; Choudhury, 1999; Yang et al., 2008, Roderick and Farquhar, 2011; Sposito, 2017) that partition P between E and Q have proven to be extremely useful in both understanding and characterising the long-term mean annual hydrological conditions in a given region.

However, the long-term mean annual hydrologic fluxes rarely occur in any given year. Instead, society must (routinely) deal with variability around the long-term mean. The classic hydro-climate extremes are droughts and floods but the key point here is that hydrologic variability is expressed on a full spectrum of time and space scales. To accommodate that perspective, we need to extend our thinking beyond the long-term mean to ask how the variability of P is partitioned into the variability of E, Q and ΔS (e.g., Orth and Destouni, 2018).

Early research on hydrologic variability focussed on extending the Budyko curve. In particular, Koster and Suarez (1999) used the Budyko curve to investigate inter-annual variability in the water cycle. In their framework, the evapotranspiration standard deviation ratio (defined as the ratio of standard deviation for E to P, σ_E/σ_P) was (also) estimated using the aridity index ($\overline{E_o}/\bar{P}$). The classic Koster and Suarez framework has been widely applied and extended in subsequent investigations of the variability in both E and Q, using catchment observations, reanalysis data and model outputs (e.g., McMahon et al., 2011; Wang and Alimohammadi 2012; Sankarasubramanian and Vogel, 2002; Zeng and Cai, 2015). However, typical applications of the Koster and Suarez framework have previously been at regional scales and there is still no comprehensive global assessment for partitioning the variability of P into the variability of E, Q and ΔS. One reason for the lack of a global comprehensive assessment is the absence of gridded global hydrologic data. Interestingly, the atmospheric science community have long used a combination of observations and model outputs to construct gridded global–scale atmospheric re-analyses and such products have become central to atmospheric research. Those atmospheric products also contain estimates of some of the key water cycle variables (e.g., P, E), such as in the widely used interim ECMWF Re-Analysis (ERA-Interim; Dee et al. 2011). Though efforts have been taken to develop land-based products from atmospheric reanalyses, e.g., ERA-Land (Balsamo et al., 2013) and MERRA-Land (Reichle et al., 2011) databases, however, the central aim of atmospheric re-analysis is to estimate atmospheric variables. That atmospheric-centric aim, understandably, ignores many of the nuances of soil water infiltration, vegetation water uptake, runoff generation and many other processes of central importance in hydrology.

Deleted: However

Deleted: ,

Deleted: which

Hydrologists have only recently accepted the challenge of developing their own re-analysis type products with perhaps the first serious hydrologic re-analysis being published as recently as a few years ago (Rodell et al., 2015). More recently, the Princeton University group has extended this early work by making available a gridded global terrestrial hydrologic re-analysis product known as the Climate Data Record (CDR) (Zhang et al., 2018). Briefly, the CDR was constructed by synthesizing multiple in-situ observations, satellite remote sensing products, and land surface model outputs to provide *gridded* estimates of global land precipitation P, evapotranspiration E, runoff Q and total water storage change ΔS (0.5° × 0.5°, monthly, 1984-2010). In developing the CDR, the authors adopted local water budget closure as the fundamental hydrologic principle. That approach presented one important difficulty. Global observations of ΔS start with the GRACE satellite mission from 2002. Hence before 2002 there is no direct observational constraint on ΔS and the authors made the further assumption that the mean annual ΔS over the full 1984-2010 period was zero at every grid-box. That is incorrect in some regions (e.g. Scanlon et al., 2018) and represents an observational problem that cannot be overcome. However, our interest is in the year-to-year variability and for that application, the assumption of no change in the mean annual ΔS over the full 1984-2010 period is unlikely to lead to major problems since we are not looking for subtle changes over time. With that caveat in mind, the aim of this study is to use this new 27-year gridded hydrologic re-analysis product to conduct an initial investigation of the inter-annual variability of the terrestrial branch of the global water cycle.

The paper is structured as follows. We begin in Section 2 by describing the various climate and hydrologic databases used in this study, and also include a further assessment of the suitability of the CDR database for this

Deleted: ing

initial variability study. In Section 3, we examine relationships between the mean and variability in the four water cycle variables (P, E, Q and ΔS). In Section 4, we first relate the variabilities to the classical aridity index and then use those results to evaluate the theory of Koster and Suarez (1999). Subsequently we examine how the variance of P is partitioned into the variances (and relevant covariances) of E, Q and ΔS and undertake an initial survey that investigates some of the factors controlling the variance partitioning. We conclude the paper with a discussion summarising what we have learnt about water cycle variability over land by using the CDR database.

Deleted: variability

2. Methods and Data

2.1 Methods

The water balance is defined by,

$$P(t) = E(t) + Q(t) + \Delta S(t) \tag{1}$$

with P the precipitation, E the evapotranspiration, Q the runoff and ΔS the total water storage change in time step t (annual in this study). By the usual variance law, we have,

$$\sigma_P^2 = \sigma_E^2 + \sigma_Q^2 + \sigma_{\Delta S}^2 + 2cov(E,Q) + 2cov(E,\Delta S) + 2cov(Q,\Delta S) \tag{2}$$

that includes all relevant variances (denoted σ^2) and covariances (denoted *cov*). Eq. (2) can be thought of as the hydrologic variance balance equation.

Deleted: Eq. (1) is the familiar hydrologic mass balance equation. In that context,

2.2 Hydrologic and Climatic Data

We use the Climate Data Record (CDR) database (Zhang et al., 2018) which is a recently released global land hydrologic re-analysis. This product includes global precipitation P, evapotranspiration E, runoff Q and water storage change ΔS (0.5° × 0.5°, monthly, 1984-2010). In this study we focus on the inter-annual variability and the monthly water cycle variables (P, E, Q and ΔS) are aggregated to annual totals. The CDR does not report additional radiation variables and we use the NASA/GEWEX Surface Radiation Budget (SRB) Release-3.0 (monthly, 1984-2007, 1° × 1°) database (Stackhouse et al., 2011) to calculate E_o (defined as the net radiation expressed as an equivalent depth of liquid water, Budyko, 1974). We then calculate the aridity index ($\overline{E_o}/\overline{P}$) using P from the CDR and E_o from the SRB databases (see Fig. S1a in the Supplementary Material).

Deleted: known here as the Climate Data Record (CDR) (Zhang et al., 2018)

In general, we anticipate two important factors, i.e., the water storage capacity and the presence of ice/snow at the surface, which are most likely to have influence on the partitioning of hydrologic variability. For the storage, the active range of the monthly water storage variation was used to approximate the water storage capacity (S_{max}). In more detail, the water storage $S(t)$ at each time step t (monthly here) was first calculated from the accumulation of $\Delta S(t)$, i.e., $S(t) = S(t\text{-}1) + \Delta S(t)$ where we assumed zero storage at the beginning of the study period (i.e., $S(0) = 0$). With the resulting time series available, S_{max} was estimated as the difference between the maximum and minimum $S(t)$ during the study period at each grid-box (see Fig. S1b in the Supplementary Material). The estimated S_{max} shows a large range from 0 to 1000 mm with the majority of values from 50 to 600 mm (Fig. S1b), which generally agrees with global rooting depth estimates assuming that water occupies from 10 to 30% of the soil volume at field capacity (Jackson et al., 1996; Wang-Erlandsson et al., 2016; Yang et al., 2016). To characterise snow/ice cover, and to distinguish extremely hot and cold regions, we also make use of a gridded global land air temperature dataset from the Climatic Research Unit (CRU TS4.01 database, monthly, 1901-2016, 0.5° × 0.5°) (Harris et al., 2014). (see Fig. S1c in the Supplementary Material).

2.3 Spatial Mask to Define Study Extent

The CDR database provides an estimate of the uncertainty (± 1σ) for each of the hydrologic variables (P, E, Q, ΔS) in each month. We use those uncertainty estimates to identify and remove regions with high relative uncertainty in the CDR data. The relative uncertainty is calculated as the ratio of root mean square of the uncertainty (± 1σ) to the mean annual P, E and Q at each grid-box following the procedure used by Milly and Dunne (2002a). Note that the long term mean ΔS is zero by construction in the CDR database, and for that reason we did not use ΔS to calculate the relative uncertainty. Grid-boxes with a relative uncertainty (in P, E and Q) of more than 10% are deemed to have high relative uncertainty (Milly and Dunne, 2002a) and were excluded from the study extent. The excluded grid-boxes were mostly in the Himalayan region, the Sahara Desert and in Greenland. The final spatial mask is shown in Fig. S2 and this has been applied throughout this study.

2.4 Further Evaluation of CDR Data for Variability Analysis

In the original work, the CDR database was validated by comparison with independent observations including (i) mean seasonal cycle of Q from 26 large basins (see Fig. 8 in Zhang et al., 2018), (ii) mean seasonal cycle of ΔS

Deleted: On

Deleted: grounds

Deleted: that

Deleted:

Deleted:

Deleted: were the water storage capacity and the presence of ice/snow at the surface from 12 large basins (Fig. 10 in Zhang et al., 2018), (iii) monthly runoff from 165 medium size basins and a further 862 small basins (Fig. 14 in Zhang et al., 2018), (iv) summer *E* from 47 flux towers (Fig. 16 in Zhang et al., 2018). Those evaluations did not directly address variability in various water cycle elements. With our focus on the variability we decided to conduct further validations of the CDR database beyond those described in the original work. In particular, we focussed on further independent assessments of *E* and we use monthly (as opposed to summer) observations of *E* from FLUXNET to evaluate the variability in *E*. We also compare the evapotranspiration *E* in the CDR with two other gridded global *E* products that were not used to develop the CDR including the LandFluxEval database (1° × 1°, monthly, 1989-2005) (Mueller et al., 2013) and the Max Planck Institute database (MPI, 0.5° × 0.5°, monthly, 1982-2011) (Jung et al., 2010). The runoff *Q* in the CDR is further compared with the gridded European *Q* product E-RUN (0.5° × 0.5°, monthly, 1951-2015) (Gudmundsson and Seneviratne, 2016).

For the comparison to FLUXNET observations (Baldocchi et al., 2001; Agarwal et al., 2010) we identified 32 flux tower sites (site locations are shown in Fig. S3 and details are shown in Table S1) having at least three years of continuous (monthly) measurements using the FluxnetLSM R package (v1.0) (Ukkola et al. 2017). The monthly totals and annual climatology of *P* and *E* from CDR generally follow FLUXNET observations, with high correlations and reasonable Root Mean Square Error (Figs. S4-S5, Table S1). Comparison of the point-based FLUXNET (~ 100 m – 1 km scale) with the grid-based CDR (~ 50 km scale) is problematic since the CDR represents an area that is at least 2500 times larger than the area represented by the individual FLUXNET towers and we anticipate that the CDR record would be "smoothed" relative to the FLUXNET record. With that in mind, we chose to compare the ratio of the standard deviation of *E* to *P* between the CDR and FLUXNET databases and this normalised comparison of the hydrologic variability proved encouraging (Fig. S6).

The comparison of *E* between the CDR and the LandFluxEval and MPI databases also proved encouraging. We found that the monthly mean *E* from the CDR database is slightly underestimated compared with LandFluxEVAL database (Fig. S7a), but agrees closely with the MPI database (Fig. S8a). In terms of variability, the standard deviations of monthly *E* from the CDR are in very close agreement with the LandFluxEVAL database (Fig. S7c), but there is a bias and scaling offset for the comparison with the MPI database particularly for the grid-cells with low standard deviation of *E* (Fig. S8c). The comparison of runoff *Q* between the E-RUN and CDR databases show that the two databases have very similar spatial patterns of both the long-term mean ($\bar{Q}$) and standard deviation

Deleted: was

(σ_Q) of the monthly Q (Fig. S10). The grid-by-grid comparison results are also encouraging, showing slight bias of both the long-term mean and standard deviation of monthly Q in the CDR database compared with the E-RUN database (Fig. S11).

Deleted:

We concluded that while the CDR database was unlikely to be perfect, it was nevertheless suitable for an initial exploratory survey of inter-annual variability in the terrestrial branch of the global water cycle.

3. Mean and Variability of Water Cycle Components

3.1 Mean Annual P, E, Q and the Budyko Curve

The global pattern of mean annual P, E, Q using the CDR data (1984-2007) is shown in Fig. 1. The mean annual P ($\bar{P}$) is prominent in tropical regions, southern China, eastern and western North America (Fig. 1a). The magnitude of mean annual E ($\bar{E}$) more or less follows the pattern of $\bar{P}$ in the tropics (Fig. 1b) while the mean annual Q ($\bar{Q}$) is particularly prominent in the Amazon, South and Southeast Asia, tropical parts of west Africa and in some other coastal regions at higher latitudes (Fig. 1c).

We relate the grid-box level ratio of $\bar{E}$ to $\bar{P}$ in the CDR database to the classical Budyko (1974) curve using the aridity index ($\overline{E_o}/\bar{P}$) (Fig. 2a). As noted previously, in the CDR database, $\overline{\Delta S}$ is forced to be zero and this enforced steady state (i.e., $\bar{P} = \bar{E} + \bar{Q}$) allowed us to also predict the ratio of $\bar{Q}$ to $\bar{P}$ using the same Budyko curve (Fig. 2b). The Budyko curves follow the overall pattern in the CDR data, which agrees with previous studies showing that the aridity index can be used to predict water availability (e.g., Gudmundsson et al., 2016). However, there is substantial scatter due to, for example, regional variations related to seasonality, water storage change and the landscape characteristics (Milly, 1994a, b, Padrón et al., 2017). With that caveat in mind, the overall patterns are as expected with $\bar{E}$ following $\bar{P}$ in dry environments ($\overline{E_o}/\bar{P} > 1.0$) while $\bar{E}$ follows $\overline{E_o}$ in wet environments ($\overline{E_o}/\bar{P} \leq 1.0$) (Fig. 2).

Deleted: trend

3.2 Inter-annual Variability in P, E, Q and ΔS

We use the variance balance equation (Eq. 2) to partition the inter-annual σ_P^2 into separate components due to σ_E^2, σ_Q^2, $\sigma_{\Delta S}^2$ along with the three covariance components ($2cov(E,Q)$, $2cov(E,\Delta S)$, $2cov(Q,\Delta S)$) (Fig. 3). The spatial pattern of σ_P^2 (Fig. 3a) is very similar to that of $\bar{P}$ (Fig. 1a), which implies that the σ_P^2 is positively correlated with $\bar{P}$. In contrast the partitioning of σ_P^2 to the various components is very different from the partitioning of $\bar{P}$ (cf. Fig. 1 and 3). First we note that while the overall spatial pattern of σ_E^2 more or less follows σ_P^2, the overall magnitude of σ_E^2 is much smaller than σ_P^2 and σ_Q^2 in most regions, and in fact σ_E^2 is also generally smaller than $\sigma_{\Delta S}^2$. The prominence of $\sigma_{\Delta S}^2$ (compared to σ_E^2) surprised us. The three covariance components ($cov(E,Q)$, $cov(E,\Delta S)$, $cov(Q,\Delta S)$) are also important in some regions. In more detail, the $cov(E,Q)$ term is prominent in regions where σ_Q^2 is large and is mostly negative in those regions (Fig. 3e), indicating that years with lower *E* are associated with higher *Q* and vice-versa. There are also a few regions with prominent positive values for $cov(E,Q)$ (e.g., the seasonal hydroclimates of northern Australia) indicating that in those regions, years with a higher *E* are associated with higher *Q*. The $cov(E,\Delta S)$ term (Fig. 3f) has a similar spatial pattern to the $cov(E,Q)$ term (Fig. 3e) but with a smaller overall magnitude. Finally, the $cov(Q,\Delta S)$ term shows a more complex spatial pattern, with both prominent positive and negative values (Fig. 3g) in regions where σ_Q^2 (Fig. 3c) and $\sigma_{\Delta S}^2$ (Fig. 3d) are both large.

These results show that the spatial patterns in variability are not simply a reflection of patterns in the long-term mean state. On the contrary, we find that of the three primary variance terms, the overall magnitude of (inter-annual) σ_E^2 is the smallest implying the least (inter-annual) variability in *E*. This is very different from the conclusions based on spatial patterns in the mean *P*, *E* and *Q* (see section 3.1). Further, while σ_Q^2 more or less follows σ_P^2 as expected, we were surprised by the magnitude of $\sigma_{\Delta S}^2$ which, in general, substantially exceeds the magnitude of σ_E^2. Further, the magnitude of the covariance terms can be important, especially in regions with high σ_Q^2. However, unlike the variances, the covariance can be both positive and negative and this introduces additional complexity. For example, with a negative covariance it is possible for the variance in *Q* (σ_Q^2) to exceed the variance in *P* (σ_P^2). To examine that in more detail we calculated the equivalent frequency distribution for each of the plots in Fig. 3. The results (Fig. S9) further emphasise that in general, σ_E^2 is the smallest of the variances (Fig. S9b). We also note that the frequency distributions for the covariances (Fig. S9efg) are not symmetrical. In summary, it is clear that spatial patterns in the inter-annual variability of the water cycle (Fig. 3) do not simply follow the spatial patterns for the inter-annual mean (Fig. 1).

3.3 Relation Between Variability and the Mean State for *P*, *E*, *Q*

Differences in the spatial patterns of the mean (Fig. 1) and inter-annual variability (Fig. 3) in the global water cycle led us to further investigate the relation between the mean and the variability for each separate component. Here we relate the standard deviation (σ_P, σ_E, σ_Q) instead of the variance to the mean of each water balance flux (Fig. 4) since the standard deviation has the same physical units as the mean making the results more comparable. As inferred previously, we find σ_P to be positively correlated with $\bar{P}$ but with substantial scatter (Fig. 4a). The same result more or less holds for the relation between σ_Q and $\bar{Q}$ (Fig. 4c). In contrast the relation between σ_E and $\bar{E}$ is very different (Fig. 4b). In particular, σ_E is a small fraction of $\bar{E}$ and this complements the earlier finding (Fig. 4b) that the inter-annual variability for *E* is generally smaller than for the other physical variables (*P*, *Q* and ΔS). (The same result was also found using both LandFluxEVAL and MPI databases, see Fig. S12 in the Supplementary Material.) Importantly, unlike *P* and *Q*, *E* is constrained by both water and energy availability (Budyko, 1974) and the limited inter-annual variability in *E* presumably reflects limited inter-annual variability in the available (radiant) energy (E_o). This is something that could be investigated in a future study.

Deleted: S10

4. Relating the Variability of Water Cycle Components to Aridity

In the previous section, we investigated spatial patterns of the mean and the variability in the global water cycle. In this section, we extend that by investigating the partitioning of σ_P^2 to the three primary physical terms (σ_E^2, σ_Q^2, $\sigma_{\Delta S}^2$) along with the three relevant covariances. For that, we begin by comparing the Koster and Suarez (1999) theory against the CDR data and then investigate how the partitioning of the variance is related to the aridity index $\overline{E_o}/\bar{P}$ (see Fig. S1a in the Supplementary Material). Following that, we investigate variance partitioning in relation to both our estimate of the storage capacity S_{max} (see Fig. S1b in the Supplementary Material) as well as the mean annual air temperature $\overline{T_a}$ (see Fig. S1c in the Supplementary Material) that we use as a surrogate for snow/ice cover. We finalise this section by examining the partitioning of variance at three selected study sites that represent extremely dry/wet, high/low water storage capacity and the hot/cold spectrums.

4.1 Comparison with the Koster and Suarez (1999) Theory

We first evaluate the classical empirical curve of Koster and Suarez (1999) by relating ratios σ_E/σ_P and σ_E/σ_P to the aridity index (Fig. 5). The ratio σ_E/σ_P in the CDR database is generally overestimated by the empirical Koster and Suarez curve, especially in dry environments (e.g., $\overline{E_o}/\overline{P}$ > 3) (Fig. 5a). The inference here is that the Koster and Suarez theory predicts σ_E/σ_P to approach unity in dry environments while the equivalent value in the CDR data is occasionally unity but is generally smaller. With σ_E/σ_P generally overestimated by the Koster and Suarez theory we expect, and find, that σ_Q/σ_P is generally underestimated by the same theory (Fig. 5b). The same overestimation was found based on the other two independent databases for E (LandFluxEVAL and MPI) (Fig. S13). This overestimation is discussed further in section 5.

Deleted: S11

4.2 Relating Inter-annual Variability to Aridity

Here we examine how the fraction of the total variance in precipitation accounted for by the three primary variance terms along with the three covariance terms varies with the aridity index ($\overline{E_o}/\overline{P}$) (Fig. 6). (Also see Fig. S14 for the spatial maps.) The ratio σ_E^2/σ_P^2 is close to zero in extremely wet regions and has an upper limit noted previously (Fig. 5a) that approaches unity in extremely dry regions (Fig. 6a). The ratio σ_Q^2/σ_P^2 is close to zero in extremely dry regions but approaches unity in extremely wet regions but with substantial scatter (Fig. 6b). The ratio $\sigma_{\Delta S}^2/\sigma_P^2$ is close to zero in both extremely dry/wet regions (Fig. 6c) and shows the largest range at an intermediate aridity index ($\overline{E_o}/\overline{P}$ ~ 1.0).

Deleted: S12

The covariance ratios are all small in extremely dry (e.g., $\overline{E_o}/\overline{P}$ ≥6.0) environments and generally show the largest range in semi-arid and semi-humid environments. The peak magnitudes for the three covariance components consistently occur when $\overline{E_o}/\overline{P}$ is close to 1.0 which is the threshold often used to separate wet and dry environments.

4.3 Further Investigations on the Factors Controlling Partitioning of the Variance

Results in the previous section demonstrated that spatial variation in the partitioning of σ_P^2 into σ_E^2, σ_Q^2, $\sigma_{\Delta S}^2$ and the three covariance components is complex (Fig. 6). To help further understand inter-annual variability of the terrestrial water cycle, we conduct further investigations in this section using two factors likely to have a major influence on the variance partitioning of σ_P^2. The first is the storage capacity $S_{\max}$ (see Fig. S1b in the Supplementary Material). The second is the mean annual air temperature $\overline{T_a}$ (see Fig. S1c in the Supplementary Material) which is used here as a surrogate for snow/ice presence.

4.3.1 Relating Inter-annual Variability to Storage Capacity

We first relate the partitioning of σ_P^2 to water storage capacity ($S_{\max}$) by repeating Fig. 6 but instead we use a logarithmic scale for the x-axis and we distinguish $S_{\max}$ via the background colour (Fig. 7). To eliminate the possible overlap of grid-cells in the colouring process, all the grid-cells over land are further separated using different latitude ranges (as shown in the four columns of Fig. 7), i.e., 90N-60N, 60N-30N, 30N-0 and 0-90S. We find that $S_{\max}$ is relatively high in wet environments ($\overline{E_o}/\overline{P} \leq 1.0$, Fig. 7a) but shows no obvious relation to the partitioning of σ_P^2. However, in dry environments ($\overline{E_o}/\overline{P} > 1.0$) the ratio σ_E^2/σ_P^2 apparently decreases with the increase of $S_{\max}$ (Fig. 7a-d). That relation is particularly obvious in extremely dry environments ($\overline{E_o}/\overline{P} \geq 6.0$) at equatorial latitudes where there is an upper limit of σ_E^2/σ_P^2 close to 1.0 when $S_{\max}$ is small (blue grid-cells in Fig. 7c). The interpretation for those extremely dry environments is that when $S_{\max}$ is small, σ_P^2 is almost completely partitioned into σ_E^2 (Fig. 7bc) with the other variance and covariance components close to zero. While for those same extremely dry environments, as $S_{\max}$ increases, the partitioning of σ_P^2 is shared between σ_E^2 and $\sigma_{\Delta S}^2$ and their covariance (Fig. 7cks) while σ_Q^2 and its covariance components remain close to zero (Fig. 7gow). However, at polar latitudes in the northern hemisphere (panels in the first and second columns of Fig. 7) there are variations that could not be easily associated with variations in $S_{\max}$ which led us to further investigate the role of snow/ice on the variance partitioning in the following section.

4.3.2 Relating Inter-annual Variability to Mean Air Temperature

To understand the potential role of snow/ice in modifying the variance partitioning, we repeat the previous analysis (Fig. 7) but here we use the mean annual air temperature ($\overline{T_a}$) to colour the grid-cells to (crudely) indicate the presence of snow/ice (Fig. 8). The results are complex and not easy to simply understand. The most important difference revealed by this analysis is in the hydrologic partitioning between cold (first column) and hot (third column) conditions in wet environments ($\overline{E_o}/\overline{P} \leq 0.5$). In particular, when $\overline{T_a}$ is high, σ_P^2 is almost completely partitioned into σ_Q^2 in wet environments (e.g., $\overline{E_o}/\overline{P} \leq 0.5$, Fig. 8g). In contrast, when $\overline{T_a}$ is low in a wet environment ($\overline{E_o}/\overline{P} \leq 0.5$ in first column of Fig. 8), there are substantial variations in the hydrologic partitioning. That result reinforces the complexity of variance partitioning in the presence of snow/ice.

4.4 Case Studies

The previous results (Section 4.3) have demonstrated that the partitioning of σ_P^2 is influenced by the water storage capacity ($S_{\max}$) in extremely dry environments ($\overline{E_o}/\overline{P}$ ≥6.0) and that the presence of snow/ice is important (as indicated by mean air temperature ($\overline{T_a}$)) in extremely wet environments ($\overline{E_o}/\overline{P}$ ≤0.5). In this section, we examine, in greater detail, several sites to gain deeper understanding of the partitioning of σ_P^2. For that purpose, we selected three sites based on extreme values for the three explanatory parameters, i.e., $\overline{E_o}/\overline{P}$ (Fig. S1a), $S_{\max}$ (Fig. S1b) and $\overline{T_a}$ (Fig. S1c). The criteria to select three climate sites are as follows, Site 1: dry ($\overline{E_o}/\overline{P} \geq 6.0$) and small $S_{\max}$ ($S_{\max}$ ≈ 0), Site 2: dry ($\overline{E_o}/\overline{P} \geq 6.0$) and relatively large $S_{\max}$ ($S_{\max} \gg 0$) and Site 3: wet ($\overline{E_o}/\overline{P} \leq 0.5$) and hot ($\overline{T_a}$ > 25 ˚C). For each of the three classes, we use a representative grid-cell (Fig. 9) to show the original time series (Fig. 10) and the partitioning of the variability (Fig. 11).

We show the P, E, Q and ΔS time series along with the relevant variances and covariances in Fig. 10. Starting with the two dry sites, at the site with low storage capacity (Site 1), the time series shows that E closely follows P leaving annual Q and ΔS close to zero (Fig. 10a). The variance of P (σ_P^2 = 206.9 mm^2) is small and almost completely partitioned into the variance of E (σ_E^2 = 196.9 mm^2), leaving very limited variance for Q, ΔS and all three covariance components (Fig. 10b). At the dry site with larger storage capacity (Site 2), E, Q and ΔS do not simply follow P (Fig. 10c). As a consequence, the variance of P (σ_P^2 = 2798.0 mm^2) is shared between E (σ_E^2 = 1150.2 mm^2), ΔS ($\sigma_{\Delta S}^2$ = 800.5 mm^2) and their covariance component ($2cov(E, \Delta S)$ = 538.4 mm^2, Fig. 10d). Switching now to the remaining wet and hot site (Site 3), we note that Q closely follows P, with ΔS close to zero and E showing little inter-annual variation (Fig. 10e). The variance of P (σ_P^2 = 57374.4 mm^2) is relatively large and almost completely partitioned into the variance of Q (σ_Q^2 = 57296.4 mm^2), leaving very limited variance for E and ΔS and the three covariance components (Fig. 10f). We also examined numerous other sites with similar extreme conditions as the three case study sites and found the same basic patterns as reported above.

To put the data from the three case study sites into a broader variability context we position the site data onto a backdrop of original Fig. 6. As noted previously, at Site 1, the ratio σ_E^2/σ_P^2 is very close to unity (Fig. 11a), and under this extreme condition, we have the following approximation,

$$\sigma_P^2 \approx \sigma_E^2 \quad \text{(Site 1, dry and } S_{\max} \approx 0\text{)} \tag{3}$$

In contrast, for Site 2 with the same aridity index but higher $S_{\max}$, we have,

$$\sigma_P^2 \approx \sigma_E^2 + \sigma_{\Delta S}^2 + 2cov(E, \Delta S) \quad \text{(Site 2, dry and } S_{\max} \gg 0) \tag{4}$$

Finally, at Site 3, we have,

$$\sigma_P^2 \approx \sigma_Q^2 \quad \text{(Site 3, wet and hot)} \tag{5}$$

4.5 Synthesis

The above simple examples demonstrate that aridity $\overline{E_o}/\bar{P}$, storage capacity $S_{\max}$ and to a lesser extent, air temperature $\overline{T_a}$, all play some role in the partitioning of σ_P^2 to the various components. Our synthesis of the results for the partitioning of σ_P^2 is summarised in Fig. 12. In dry environments with low storage capacity ($S_{\max} \approx 0$) we have minimal runoff and expect that σ_P^2 is more or less completely partitioned into σ_E^2 (Fig. 12a). In those environments, (inter-annual) variations in storage $\sigma_{\Delta S}^2$ play a limited role in setting the overall variability. However, in dry environments with larger storage capacity ($S_{\max} \gg 0$), σ_E^2 is only a small fraction of σ_P^2 (Fig. 12a) leaving most of the overall variance in σ_P^2 to be partitioned to $\sigma_{\Delta S}^2$ and the covariance between E and ΔS (Fig. 12c and Fig. 12e). This emphasises the hydrological importance of water storage capacity in buffering variations of the water cycle under dry conditions.

Under extremely wet conditions, the largest difference in variance partitioning is not due to differences in storage capacity but is instead related to differences in mean air temperature. In wet and hot environments, we have maximum runoff and find that σ_P^2 is more or less completely partitioned into σ_Q^2 (Fig. 12b) while the partitioning to σ_E^2 and $\sigma_{\Delta S}^2$ is small. However, in wet and cold environments, the variance partitioning shows great complexity with σ_P^2 being partitioned into all possible components. We suggest that this emphasises the hydrological importance of thermal processes (melting/freezing) under extremely cold conditions.

However, the most complex patterns to interpret are those for semi-arid to semi-humid environments (i.e., $\overline{E_o}/\bar{P}$ ~1.0). Despite a multitude of attempts over an extended period we were unable to develop a simple useful synthesis to summarise the partitioning of variability in those environments. We found that the three covariance terms all play important roles and we also found that simple environmental gradients (e.g., dry/wet, high/low storage capacity, hot/cold) could not easily explain the observed patterns. We anticipate that vegetation related processes (e.g., phenology, rooting depth, gas exchange characteristics, disturbance, etc.) may prove to be important in explaining hydrologic variability in these biologically productive regions that support most of human population. This result implies that a major scientific effort will be needed to develop a synthesis of the controlling factors for variability of the water cycle in these environments.

5. Discussion and Conclusions

Importantly, hydrologists have long been interested in hydrologic variability, but without readily available databases it has been difficult to quantify water cycle variability. For example, we are not aware of maps showing global spatial patterns in variance for any terms of the water balance (except for *P*). In this study, we describe an initial investigation of the inter-annual variability of the terrestrial branch in the global water cycle that uses the recently released global monthly Climate Data Record (CDR) database for *P*, *E*, *Q* and ΔS. The CDR is one of the first dedicated hydrologic reanalysis databases and includes data for a 27-year period. Accordingly, we could only examine hydrologic variability over this relatively short period. Further, we expect future improvements and modifications as the hydrologic community seeks to further develop and refine these new reanalysis databases. With those caveats in mind, we started this analysis by first investigating the partitioning of *P* in the water cycle in terms of long-term mean and then extended that to the inter-annual variability using a theoretical variance balance equation (Eq. 2). Despite the initial nature of this investigation we have been able to establish some useful general principles.

The mean annual *P* is mostly partitioned into mean annual *E* and *Q*, as is well known, and the results using the CDR were generally consistent with the earlier Budyko framework (Fig. 2). Having established that, the first general finding is that the spatial pattern in the partitioning of inter-annual variability in the water cycle is not simply a reflection of the spatial pattern in the partitioning of the long-term mean. In particular, with the variance calculations, the annual anomalies are squared and hence the storage anomalies do not cancel out like they do when calculating the mean. With that in mind, we were surprised that the inter-annual variability of water storage change ($\sigma_{\Delta S}^2$) is typically larger than the inter-annual variability of evapotranspiration (σ_E^2) (cf. Fig. 3b and 3d). The consequence is that $\sigma_{\Delta S}^2$ is more important than σ_E^2 for understanding inter-annual variability of global water cycle. A second important generalisation is that unlike the variance components which are all positive, the three covariance components in the theory (Eq. 2) can be both positive and negative. We report results here showing both large positive and negative values for the three covariance terms (Fig. 3efg). This was especially prevalent in biologically productive regions ($0.5<\overline{E_o}/\overline{P}<1.5$, Fig. 3eg). When examining the mean state, we are accustomed to think that P sets a limit to E, Q and ΔS, as per the mass balance (Eq. 1). But the same thinking does not extend to the variance balance since the covariance terms on the right hand side of Eq. 2 can be both large and negative leading to circumstances where the variability in the sinks (σ_E^2, σ_Q^2, $\sigma_{\Delta S}^2$) could actually exceed variability in the source (σ_P^2). These general principles of variance partitioning in the water cycle above may vary at different time scales (e.g., monthly, daily), and we expect more details of the variability partitioning across various temporal scales to be investigated in future studies.

Deleted: propagation

Deleted: the

Our initial attempt to develop deeper understanding of variance partitioning was based on a series of case studies located in extreme environments (wet/dry vs hot/cold vs high/low water storage capacity). The results offered some further insights about hydrologic variability. For example, under extremely dry (water-limited) environments, with limited storage capacity (S_{max}) we found that E follows P and σ_E^2 follows σ_P^2, with σ_Q^2 and $\sigma_{\Delta S}^2$ both approaching zero. However, as S_{max} increases, the partitioning of σ_P^2 progressively shifts to a balance between σ_E^2, $\sigma_{\Delta S}^2$ and cov(E, ΔS) (Figs. 10-12). This result explains the overestimation of σ_E/σ_P by the empirical theory of Koster and Suarez (1999) which implicitly assumed no inter-annual change in storage. The Koster and Suarez empirical theory is perhaps better described as an upper limit that is based on minimal storage capacity, and that any increase in storage capacity would promote the partitioning of σ_P^2 to $\sigma_{\Delta S}^2$ particularly under dry conditions (Figs. 10-12).

In extremely wet/hot environments (i.e., no snow/ice presence) we found σ_P^2 to be mostly partitioned to σ_Q^2 (with both σ_E^2 and $\sigma_{\Delta S}^2$ approaching zero, Fig. 10). In contrast, in extremely wet/cold environments, the partitioning of σ_P^2 was highly (spatially) variable presumably because of spatial variability in the all-important thermal processes (freeze/melt).

The most complex results were found in mesic biologically productive environments (0.5<$\overline{E_o}/\overline{P}$ <1.5), where all three covariance terms (Eq. 2) were found to be relatively large and therefore they all played critical roles in the overall partitioning of variability (Fig. 6). As noted above, in many of these regions, the (absolute) magnitudes of the covariances were actually larger than the variances of the water balance components E, Q and ΔS (e.g., Fig. 3). That result demonstrates that deeper understanding of the process-level interactions that are embedded within each of the three covariance terms (e.g., the role of seasonal vegetation variation) will be needed to develop process-based understanding of variability in the water cycle in these biologically productive regions (0.5<$\overline{E_o}/\overline{P}$ <1.5).

The syntheses of the long-term mean water cycle originated in 1970s (Budyko, 1974), and it took several decades for those general principles to become widely adopted in the hydrologic community. The hydrologic data needed to understand hydrologic variability are only now becoming available. With those data we can begin to develop a process-based understanding of hydrologic variability that can be used for a variety of purposes, e.g., deeper understanding of hydro-climatic behaviour, hydrologic risk analysis, climate change assessments and hydrologic sensitivity studies are just a few applications that spring to mind. The initial results presented here show that a major intellectual effort will be needed to develop a general understanding of hydrologic variability.

Acknowledgements

This research was supported by the Australian Research Council (CE11E0098, CE170100023), and D.Y. also acknowledges support by the National Natural Science Foundation of China (51609122). We thank Dr Anna Ukkola for help in accessing the FLUXNET database. We thank the reviewers (including Dr René Orth and two anonymous reviewers) for helpful comments that improved the manuscript. The authors declare that there is no conflict of interests regarding the publication of this paper. All data used in this paper are available online as referenced in the 'Methods and Data' section.

References

Agarwal, D. A., Humphrey, M., Beekwilder, N. F., Jackson, K. R., Goode, M. M., and van Ingen, C.: A data-centered collaboration portal to support global carbon-flux analysis, Concurr. Comp-Pract. E., 22, 2323-2334, https://doi.org/10.1002/cpe.1600, 2010.

Baldocchi, D., Falge, E., Gu, L., Olson, R., Hollinger, D., Running, S., Anthoni, P., Bernhofer, C., Davis, K., Evans, R., Fuentes, J., Goldstein, A., Katul, G., Law, B., Lee, X., Malhi, Y., Meyers, T., Munger, W., Oechel, W., Paw U, K. T., Pilegaard, K., Schmid, H. P., Valentini, R., Verma, S., Vesala, T., Wilson, K., and Wofsy, S.: FLUXNET: A New Tool to Study the Temporal and Spatial Variability of Ecosystem-Scale Carbon Dioxide, Water Vapor, and Energy Flux

Densities, B. Am. Meteorol. Soc., 82, 2415-2434, https://doi.org/10.1175/1520-0477(2001)082<2415:FANTTS>2.3.CO;2, 2001.

Balsamo, G., Albergel, C., Beljaars, A., Boussetta, S., Brun, E., Cloke, H., Dee, D., Dutra, E., Muñoz-Sabater, J., Pappenberger, F., de Rosnay, P., Stockdale, T., and Vitart, F.: ERA-Interim/Land: a global land surface reanalysis data set, Hydrol. Earth Syst. Sci., 19, 389-407, 10.5194/hess-19-389-2015, 2015.

Budyko, M. I.: Climate and Life. Academic Press, London, 1974.

Choudhury, B. J.: Evaluation of an empirical equation for annual evaporation using field observations and results from a biophysical model, J. Hydrol., 216, 99-110, https://doi.org/10.1016/S0022-1694(98)00293-5, 1999.

Dee, D. P., Uppala, S. M., Simmons, A. J., Berrisford, P., Poli, P., Kobayashi, S., Andrae, U., Balmaseda, M. A., Balsamo, G., Bauer, P., Bechtold, P., Beljaars, A. C. M., van de Berg, L., Bidlot, J., Bormann, N., Delsol, C., Dragani, R., Fuentes, M., Geer, A. J., Haimberger, L., Healy, S. B., Hersbach, H., Hólm, E. V., Isaksen, L., Kållberg, P., Köhler, M., Matricardi, M., McNally, A. P., Monge-Sanz, B. M., Morcrette, J. J., Park, B. K., Peubey, C., de Rosnay, P., Tavolato, C., Thépaut, J. N., and Vitart, F.: The ERA-Interim reanalysis: configuration and performance of the data assimilation system, Q. J. R. Meteorol. Soc., 137, 553-597, https://doi.org/10.1002/qj.828, 2011.

Donohue, R. J., Roderick, M. L., and McVicar, T. R.: Can dynamic vegetation information improve the accuracy of Budyko's hydrological model?, J. Hydrol., 390, 23-34, https://doi.org/10.1016/j.jhydrol.2010.06.025, 2010.

Fu, B. P.: On the Calculation of the Evaporation from Land Surface, Sci. Atmos. Sin., 5, 23-31, 1981.

Gudmundsson, L., Greve, P., and Seneviratne, S. I.: The sensitivity of water availability to changes in the aridity index and other factors—A probabilistic analysis in the Budyko space, Geophys. Res. Lett., 43, 6985-6994, https://doi.org/10.1002/2016GL069763, 2016.

Gudmundsson, L., and Seneviratne, S. I.: Observation-based gridded runoff estimates for Europe (E-RUN version 1.1), Earth Syst. Sci. Data, 8, 279-295, 10.5194/essd-8-279-2016, 2016.

Harris, I., Jones, P. D., Osborn, T. J., and Lister, D. H.: Updated high-resolution grids of monthly climatic observations–the CRU TS3. 10 Dataset, Int. J. Climatol., 34, 623-642, https://doi.org/10.1002/joc.3711, 2014.

Huning, L. S., and AghaKouchak, A.: Mountain snowpack response to different levels of warming, Proc. Natl. Acad. Sci. U. S. A., 115, 10932, https://doi.org/10.1073/pnas.1805953115, 2018.

Jackson, R. B., Canadell, J., Ehleringer, J. R., Mooney, H. A., Sala, O. E., and Schulze, E. D.: A Global Analysis of Root Distributions for Terrestrial Biomes, Oecologia, 108, 389-411, https://doi.org/10.1007/BF00333714, 1996.

Jung, M., Reichstein, M., Ciais, P., Seneviratne, S. I., Sheffield, J., Goulden, M. L., Bonan, G., Cescatti, A., Chen, J., de Jeu, R., Dolman, A. J., Eugster, W., Gerten, D., Gianelle, D., Gobron, N., Heinke, J., Kimball, J., Law, B. E., Montagnani, L., Mu, Q., Mueller, B., Oleson, K., Papale, D., Richardson, A. D., Roupsard, O., Running, S., Tomelleri, E., Viovy, N., Weber, U., Williams, C., Wood, E., Zaehle, S., and Zhang, K.: Recent decline in the global land evapotranspiration trend due to limited moisture supply, Nature, 467, 951, https://doi.org/10.1038/nature09396, 2010.

Koster, R. D., and Suarez, M. J.: A Simple Framework for Examining the Interannual Variability of Land Surface Moisture Fluxes, J. Clim., 12, 1911-1917, https://doi.org/10.1175/1520-0442(1999)012<1911:ASFFET>2.0.CO;2, 1999.

McMahon, T. A., Peel, M. C., Pegram, G. G. S., and Smith, I. N.: A Simple Methodology for Estimating Mean and Variability of Annual Runoff and Reservoir Yield under Present and Future Climates, J. Hydrometeorol., 12, 135-146, https://doi.org/10.1175/2010jhm1288.1, 2011.

Milly, P. C. D.: Climate, soil water storage, and the average annual water balance, Water Resour. Res., 30, 2143-2156, https://doi.org/10.1029/94WR00586, 1994a.

Milly, P. C. D.: Climate, interseasonal storage of soil water, and the annual water balance, Adv. Water Resour., 17, 19-24, https://doi.org/10.1016/0309-1708(94)90020-5, 1994b.

Milly, P. C. D., and Dunne, K. A.: Macroscale water fluxes 1. Quantifying errors in the estimation of basin mean precipitation, Water Resour. Res., 38, 23-21-23-14, https://doi.org/10.1029/2001WR000759, 2002a.

Milly, P. C. D., and Dunne, K. A.: Macroscale water fluxes 2. Water and energy supply control of their interannual variability, Water Resour. Res., 38, 24-21-24-29, https://doi.org/10.1029/2001WR000760, 2002b.

Mueller, B., Hirschi, M., Jimenez, C., Ciais, P., Dirmeyer, P. A., Dolman, A. J., Fisher, J. B., Jung, M., Ludwig, F., Maignan, F., Miralles, D. G., McCabe, M. F., Reichstein, M., Sheffield, J., Wang, K., Wood, E. F., Zhang, Y., and Seneviratne, S. I.: Benchmark products for land evapotranspiration: LandFlux-EVAL multi-data set synthesis, Hydrol. Earth. Syst. Sci., 17, 3707-3720, https://doi.org/10.5194/hess-17-3707-2013, 2013.

Norby, R. J., Ledford, J., Reilly, C. D., Miller, N. E., and O'Neill, E. G.: Fine-root production dominates response of a deciduous forest to atmospheric CO2 enrichment, Proc. Natl. Acad. Sci. U. S. A., 101, 9689-9693, https://doi.org/10.1073/pnas.0403491101, 2004.

Orth, R., and Destouni, G.: Drought reduces blue-water fluxes more strongly than green-water fluxes in Europe, Nat. Commun., 9, 3602, https://doi.org/10.1038/s41467-018-06013-7, 2018.

Padrón, R. S., Gudmundsson, L., Greve, P., and Seneviratne, S. I.: Large-Scale Controls of the Surface Water Balance Over Land: Insights From a Systematic Review and Meta-Analysis, Water Resources Research, 53, 9659-9678, 10.1002/2017WR021215, 2017.

Reichle, R. H., Koster, R. D., De Lannoy, G. J. M., Forman, B. A., Liu, Q., Mahanama, S. P. P., and Touré, A.: Assessment and Enhancement of MERRA Land Surface Hydrology Estimates, Journal of Climate, 24, 6322-6338, 10.1175/JCLI-D-10-05033.1, 2011.

Rodell, M., Beaudoing, H. K., L'Ecuyer, T. S., Olson, W. S., Famiglietti, J. S., Houser, P. R., Adler, R., Bosilovich, M. G., Clayson, C. A., Chambers, D., Clark, E., Fetzer, E. J., Gao, X., Gu, G., Hilburn, K., Huffman, G. J., Lettenmaier, D. P., Liu, W. T., Robertson, F. R., Schlosser, C. A., Sheffield, J., and Wood, E. F.: The Observed State of the Water Cycle in the Early Twenty-First Century, J. Clim., 28, 8289-8318, https://doi.org/10.1175/JCLI-D-14-00555.1, 2015.

Roderick, M. L., and Farquhar, G. D.: A simple framework for relating variations in runoff to variations in climatic conditions and catchment properties, Water Resour. Res., 47, https://doi.org/10.1029/2010WR009826, 2011.

Sankarasubramanian, A., and Vogel, R. M.: Annual hydroclimatology of the United States, Water Resour. Res., 38, 19-11-19-12, https://doi.org/10.1029/2001WR000619, 2002.

Scanlon, B. R., Zhang, Z., Save, H., Sun, A. Y., Müller Schmied, H., van Beek, L. P. H., Wiese, D. N., Wada, Y., Long, D., Reedy, R. C., Longuevergne, L., Döll, P., and Bierkens, M. F. P.: Global models underestimate large decadal declining and rising water storage trends relative to GRACE satellite data, Proc. Natl. Acad. Sci. U. S. A., https://doi.org/10.1073/pnas.1704665115, 2018.

Sposito, G.: Understanding the Budyko Equation, Water, 9, https://doi.org/10.3390/w9040236, 2017.

Stackhouse, P. W., Gupta, S. K., Cox, S. J., Mikovitz, J. C., Zhang, T., and Hinkelman, L. M.: The NASA/GEWEX Surface Radiation Budget Release 3.0: 24.5-Year Dataset. In: GEWEX News, No. 1, 2011.

Ukkola, A. M., Haughton, N., De Kauwe, M. G., Abramowitz, G., and Pitman, A. J.: FluxnetLSM R package (v1.0): a community tool for processing FLUXNET data for use in land surface modelling, Geosci. Model. Dev., 10, 3379-3390, https://doi.org/10.5194/gmd-10-3379-2017, 2017.

Wang, D., and Alimohammadi, N.: Responses of annual runoff, evaporation, and storage change to climate variability at the watershed scale, Water Resour. Res., 48, https://doi.org/10.1029/2011WR011444, 2012.

Wang-Erlandsson, L., Bastiaanssen, W. G. M., Gao, H., Jägermeyr, J., Senay, G. B., van Dijk, A. I. J. M., Guerschman, J. P., Keys, P. W., Gordon, L. J., and Savenije, H. H. G.: Global root zone storage capacity from satellite-based evaporation, Hydrol. Earth Syst. Sci., 20, 1459-1481, https://doi.org/10.5194/hess-2015-533, 2016.

Yang, H., Yang, D., Lei, Z., and Sun, F.: New analytical derivation of the mean annual water-energy balance equation, Water Resour. Res., 44, https://doi.org/10.1029/2007WR006135, 2008.

Yang, Y., Donohue, R. J., and McVicar, T. R.: Global estimation of effective plant rooting depth: Implications for hydrological modeling, Water Resour. Res., 52, 8260-8276, https://doi.org/10.1002/2016WR019392, 2016.

Zeng, R., and Cai, X.: Assessing the temporal variance of evapotranspiration considering climate and catchment storage factors, Adv. Water Resour., 79, 51-60, https://doi.org/10.1016/j.advwatres.2015.02.008, 2015.

Zhang, L., Potter, N., Hickel, K., Zhang, Y., and Shao, Q.: Water balance modeling over variable time scales based on the Budyko framework – Model development and testing, J. Hydrol., 360, 117-131, https://doi.org/10.1016/j.jhydrol.2008.07.021, 2008.

Zhang, Y., Pan, M., Sheffield, J., Siemann, A. L., Fisher, C. K., Liang, M. L., Beck, H. E., Wanders, N., MacCracken, R. F., Houser, P. R., Zhou, T., Lettenmaier, D. P., Ma, Y., Pinker, R. T., Bytheway, J., Kummerow, C. D., and Wood, E. F.: A Climate Data Record (CDR) for the global terrestrial water budget: 1984-2010, Hydrol. Earth Syst. Sci., 22, 241-263, https://doi.org/10.5194/hess-22-241-2018, 2018.

List of Figures:

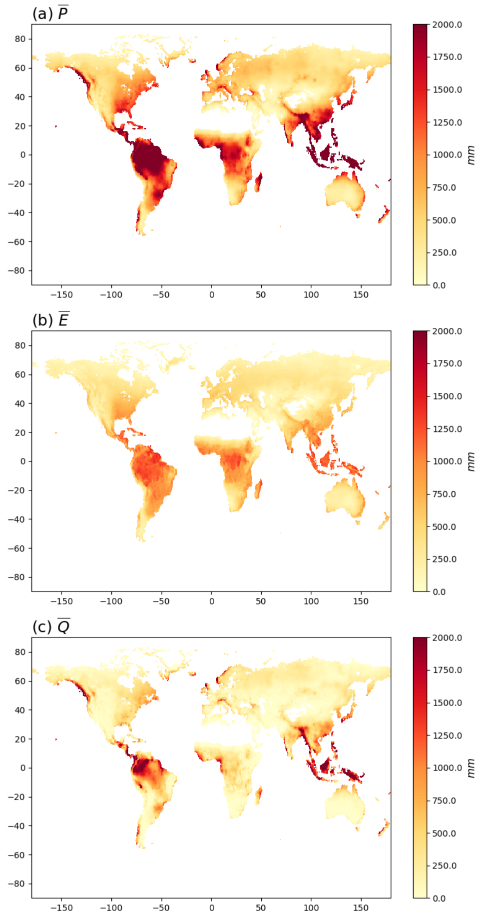

Figure 1. Mean annual (1984-2010) (a) P, (b) E and (c) Q. Note that the mean annual ΔS in the CDR database is zero by construction and is not shown.

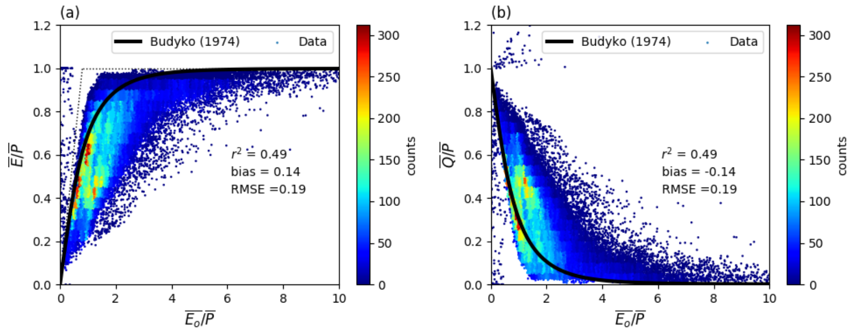

Figure 2. Relationship of mean annual (a) evapotranspiration ($\overline{E}/\overline{P}$) and (b) runoff ($\overline{Q}/\overline{P}$) ratios to the aridity index ($\overline{E_o}/\overline{P}$) from the CDR and SRB databases. For comparison, the Budyko (1974) curve is shown on the left panel (Fig. 2a). The curve on the right panel (Fig. 2b) is calculated assuming a steady state ($\overline{Q}/\overline{P} = 1 - \overline{E}/\overline{P}$).

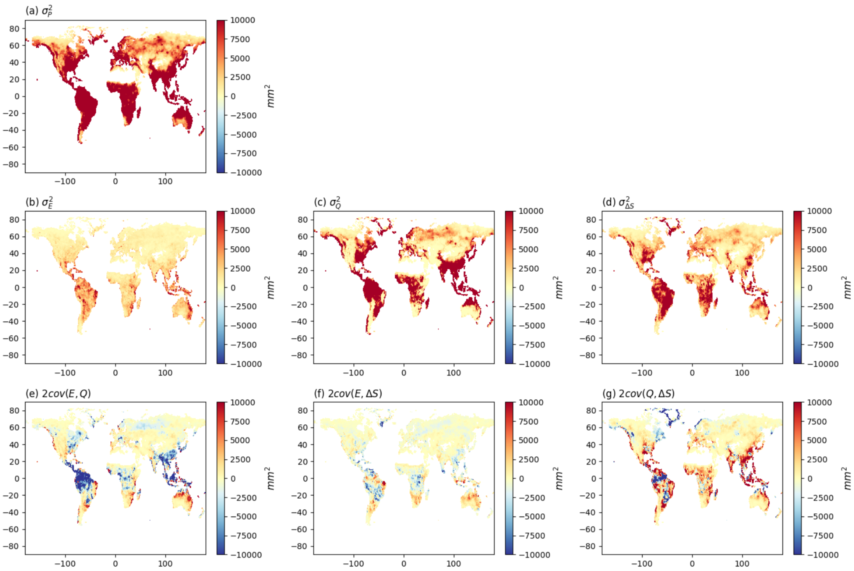

Figure 3. Water cycle variances (σ_P^2, σ_E^2, σ_Q^2, $\sigma_{\Delta S}^2$) and covariances ($cov(E, Q)$, $cov(E, \Delta S)$, $cov(Q, \Delta S)$). Note that we have multiplied the covariances by two (see Eq. 2).

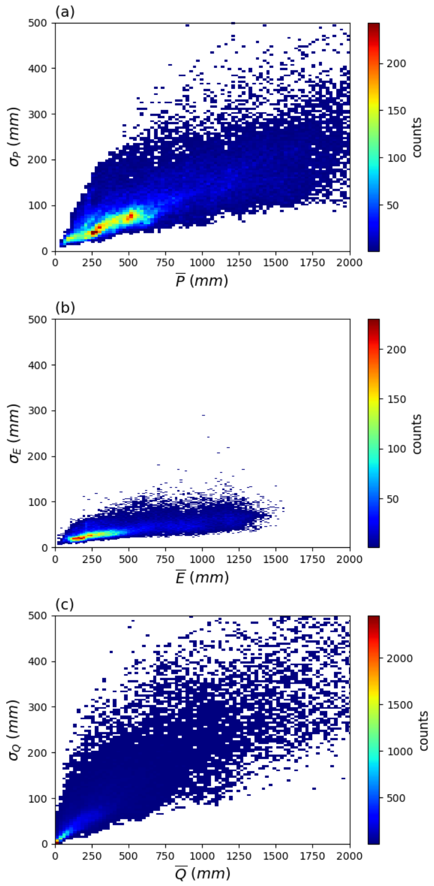

Figure 4. Relation between inter-annual mean and standard deviation for (a) *P*, (b) *E* and (c) *Q* from the CDR database. Note that the mean annual ΔS is zero by construction and is not shown.

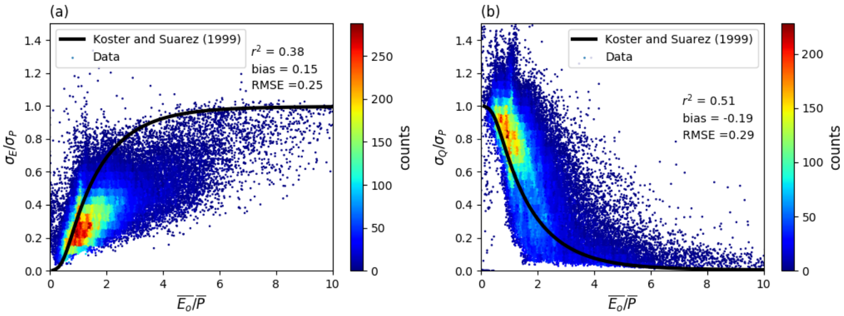

Figure 5. Relationship of inter-annual standard deviation of (a) evapotranspiration (σ_E/σ_P) and (b) runoff (σ_Q/σ_P) ratios to aridity ($\overline{E_o}/\overline{P}$). The curves represent the semi-empirical relations from Koster and Suarez (1999).

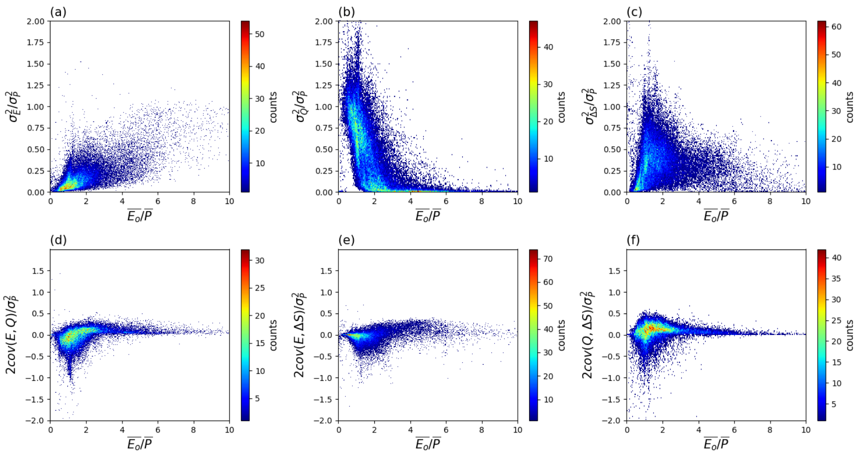

Figure 6. Relation between water cycle variances-covariances (see Fig. 3b-g) as a fraction of the variance of P (σ_P^2) and the aridity index ($\overline{E_o}/\overline{P}$) coloured by density. Note that we have multiplied the covariance components by two (see Eq. 2).

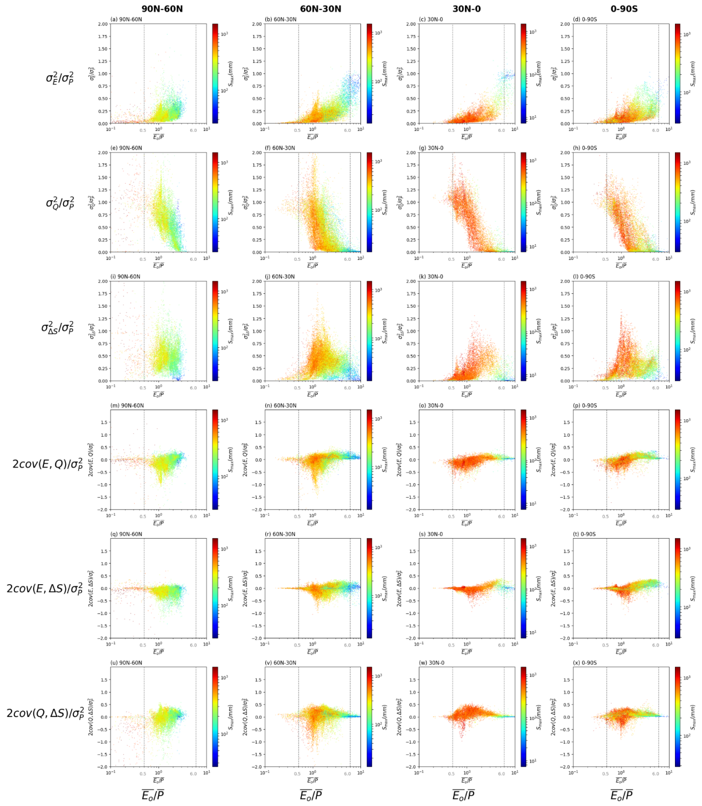

Figure 7. Relation between water cycle variances-covariances (see Fig. 3b-g) as a fraction of the variance for P (σ_P^2) and the aridity index ($\overline{E_o}/\overline{P}$) for grid-cells over different latitude ranges (i.e., 90N-60N, 60N-30N, 30N-0 and 0-90S). The colours relate to the water storage capacity S_{max}. Note that we have multiplied the covariances by two (see Eq. 2). The vertical grey dashed lines represent thresholds used to separate extremely dry ($\overline{E_o}/\overline{P} \geq 6.0$) and wet ($\overline{E_o}/\overline{P} \leq 0.5$) environments. Note the use of a logarithmic x-axis and scale bar for S_{max}.

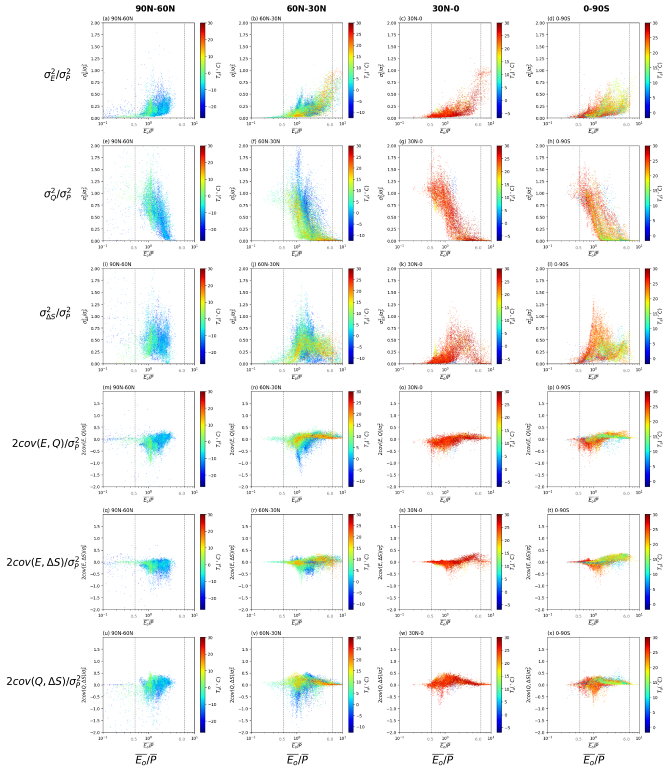

Figure 8. Relation between water cycle variances-covariances (see Fig. 3b-g) as a fraction of the variance for P (σ_P^2) and the aridity index ($\overline{E_o}/\overline{P}$) for grid-cells over different latitude ranges (i.e., 90N-60N, 60N-30N, 30N-0 and 0-90S). The colours relate to the mean air temperature ($\overline{T_a}$). Note that we have multiplied the covariances by two (see Eq. 2). The vertical grey dashed lines represent thresholds used to separate extremely dry ($\overline{E_o}/\overline{P} \geq 6.0$) and wet ($\overline{E_o}/\overline{P} \leq 0.5$) environments.

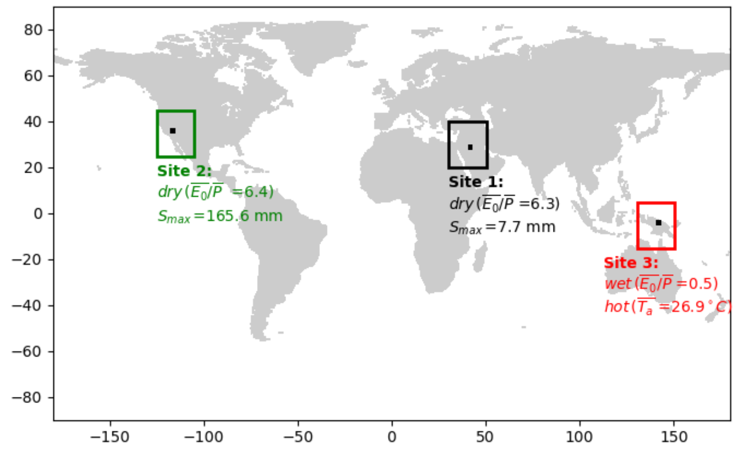

Figure 9. Locations of three representative grid-cells used as case study sites.

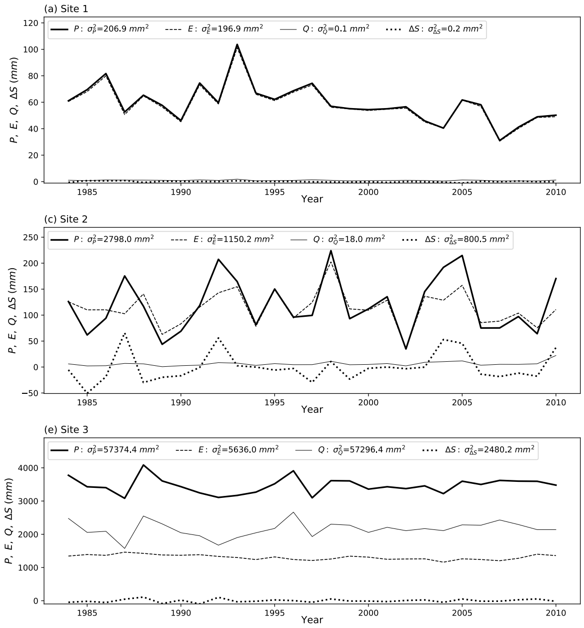

(b) Variance-covariance matrix (Site 1, unit: mm^2)

	E	Q	ΔS
E	196.9	3.4	1.5
Q	3.4	0.1	0.0
ΔS	1.5	0.0	0.2
Inter-annual variance of P : 206.9			

*Note: The values along the diagonal of each line are variance values for E, Q, and ΔS, and other values are covariance values between the two crossed components.

(d) Variance-covariance matrix (Site 2, unit: mm^2)

	E	Q	ΔS
E	1150.2	71.2	269.2
Q	71.2	18.0	74.3
ΔS	269.2	74.3	800.5
Inter-annual variance of P : 2798.0			

(f) Variance-covariance matrix (Site 3, unit: mm^2)

	E	Q	ΔS
E	5636.0	-4548.6	651.7
Q	-4548.6	57296.4	-122.2
ΔS	651.7	-122.2	2480.2
Inter-annual variance of P : 57374.4			

Figure 10. Inter-annual time series (*P*, *E*, *Q* and Δ*S*) and the associated variance-covariance matrix (*E*, *Q* and Δ*S*) for case study Sites 1-3. Left column shows time series for (a) Site 1, (c) Site 2 and (e) Site 3, with right column i.e., (b), (d) and (f), the associated variance-covariance matrix for three sites. Note that the covariance values in the tables should be multiplied by two to agree with the variance-covariance balance in Eq. (2).

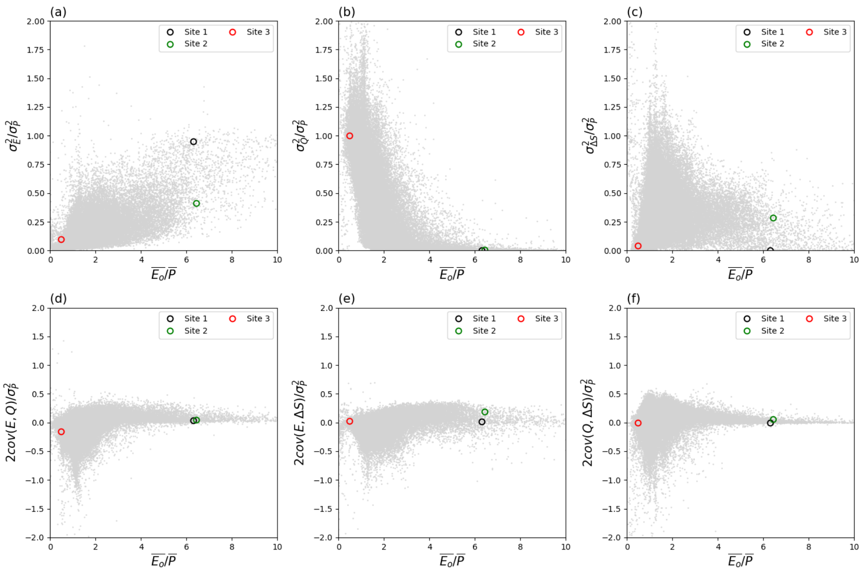

Figure 11. Location of three case study sites in the water cycle variability space. The grey background dots are from Fig. 6.

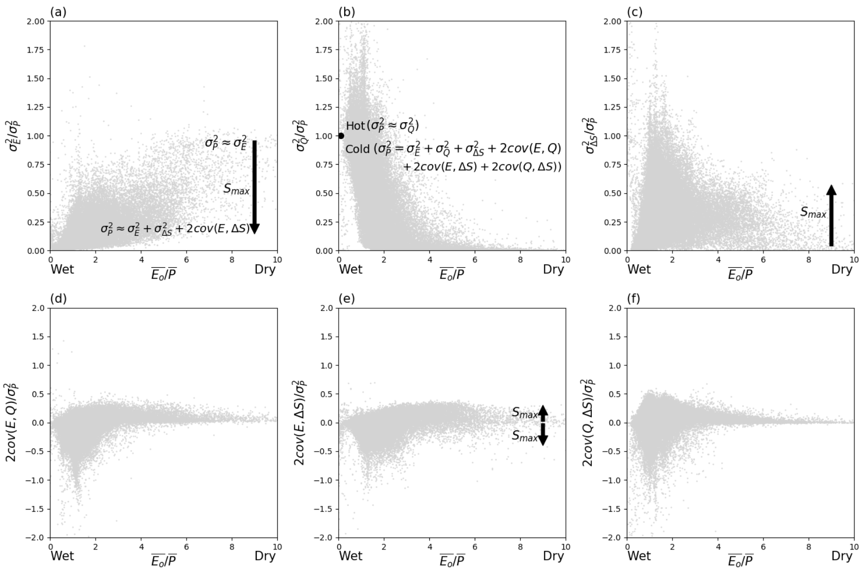

Figure 12. Synthesis of factors controlling variance partitioning. The arrows denote trends with increasing S_{max}. The grey background dots are from Fig. 6.

Inter-annual variability of the global terrestrial water cycle

Dongqin Yin[1,2], Michael L. Roderick[1,3]

[1] Research School of Earth Sciences, Australian National University, Canberra, ACT, 2601, Australia

[2]Australian Research Council Centre of Excellence for Climate System Science, Canberra, ACT, 2601, Australia

[3]Australian Research Council Centre of Excellence for Climate Extremes, Canberra, ACT, 2601, Australia

Supplementary Material

This Supplementary Material contains Figures S1-S14 and Table S1.

Deleted: S12

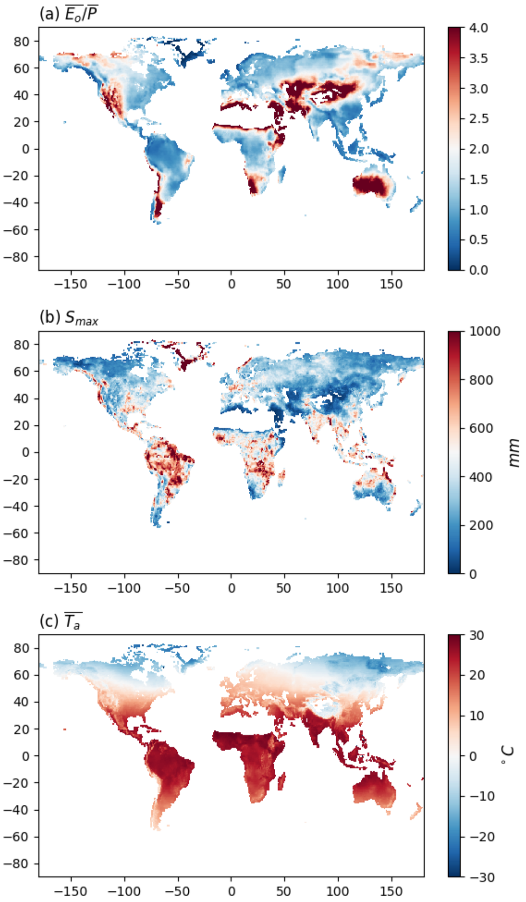

Figure S1. (a) Aridity index ($\overline{E_o}/\overline{P}$), (b) water storage capacity (S_{max}) and (c) mean annual air temperature ($\overline{T_a}$) used in the analysis.

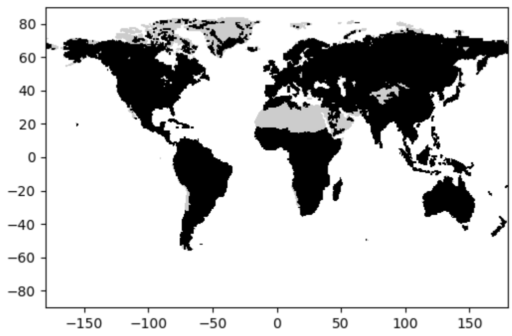

Figure S2. Spatial mask used in this study. Grey areas (e.g., Himalayan region, Sahara Desert, Greenland) have been masked out of the CDR database.

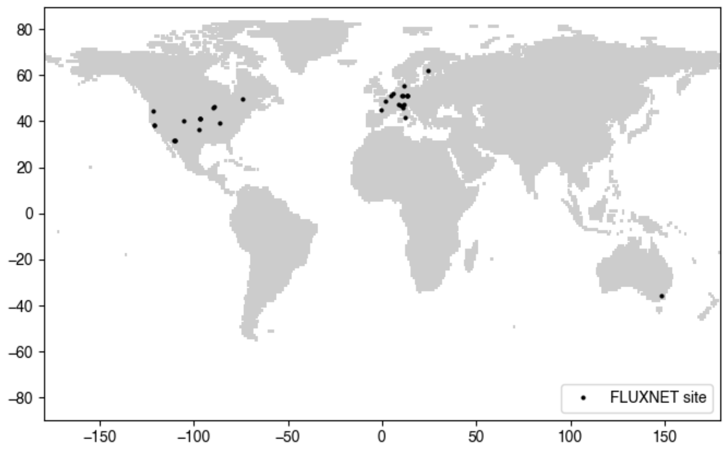

Figure S3. Location of the 32 FLUXNET sites used to evaluate the Climate Data Record (CDR).

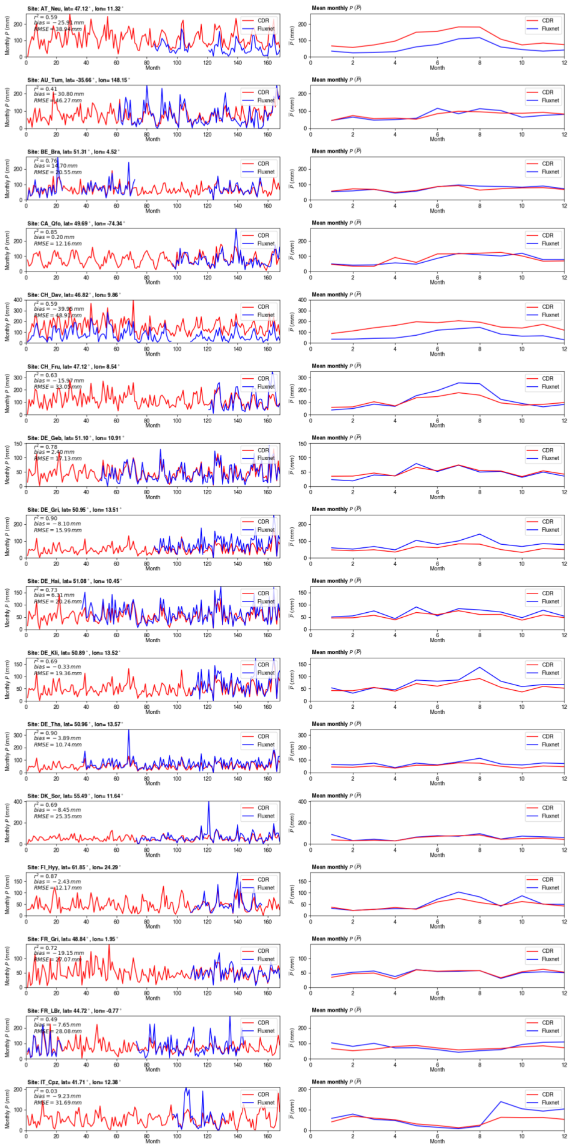

Figure S4. Comparison of monthly precipitation *P* time series (left panels) and mean monthly *P* (right panels) between FLUXNET observations at 32 sites (Table S1) and the Climate Data Record (CDR).

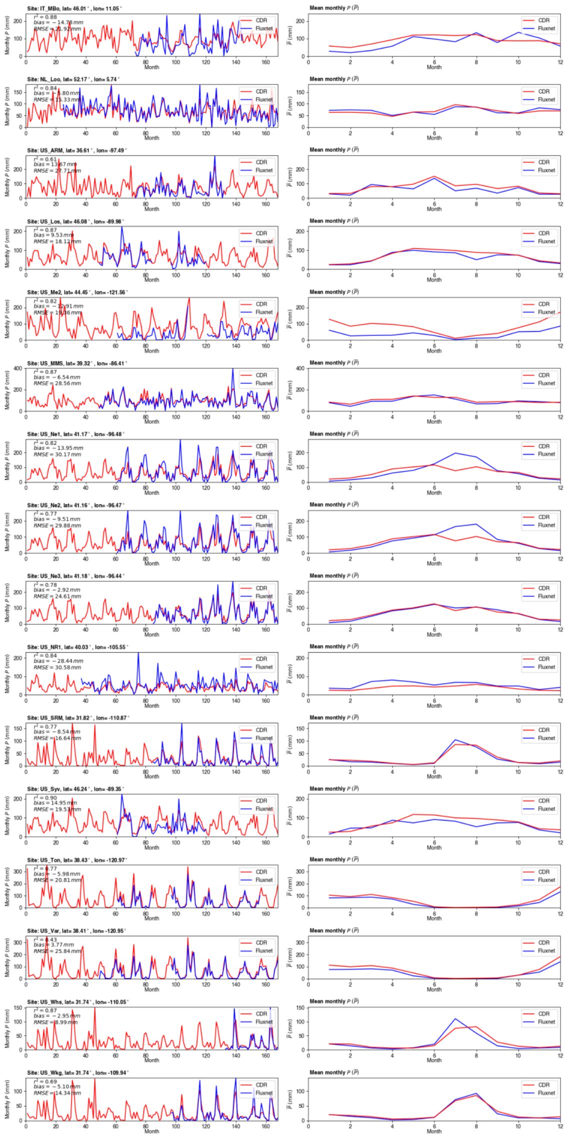

Figure S4 continued.

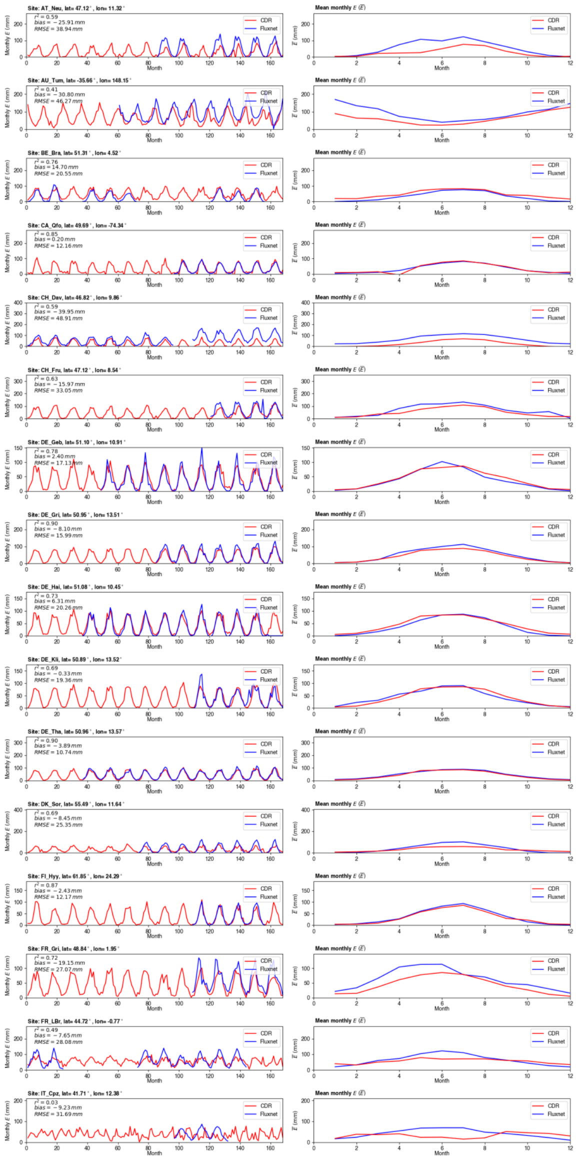

Figure S5. Comparison of monthly evapotranspiration *E* time series (left panels) and mean monthly *E* (right panels) between FLUXNET site observations and the Climate Data Record (CDR).

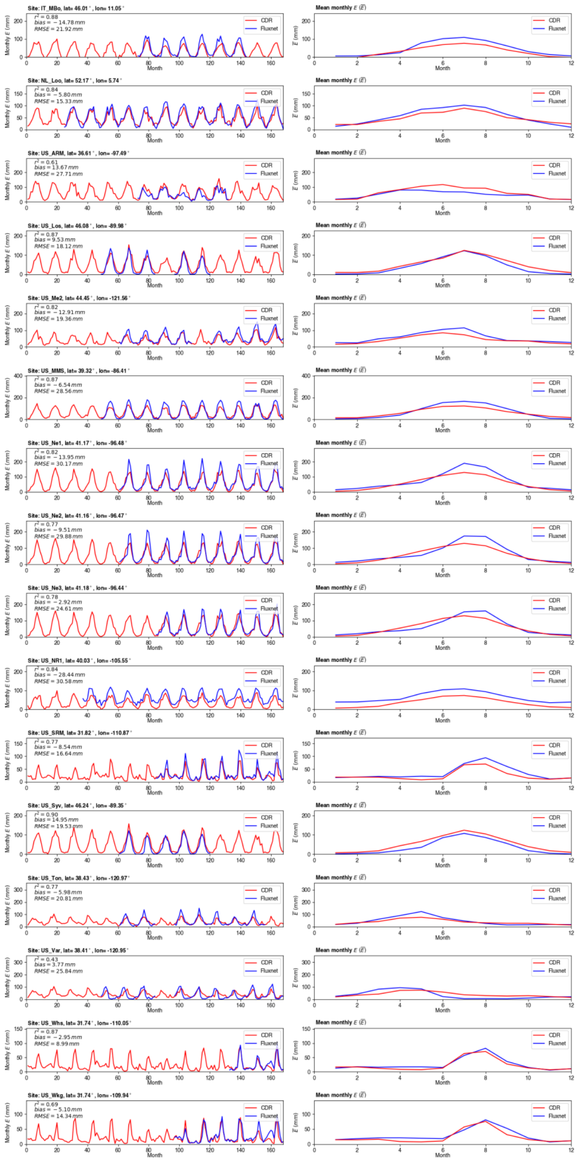

Figure S5 continued.

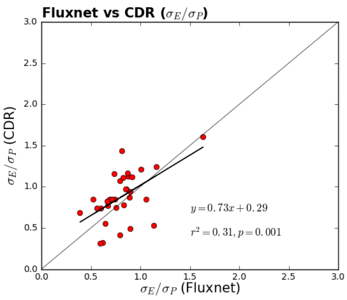

Figure S6. Comparison of ratio of standard deviation of monthly evapotranspiration *E* to precipitation *P* (σ_E/σ_P) between FLUXNET site observations and the Climate Data Record (CDR).

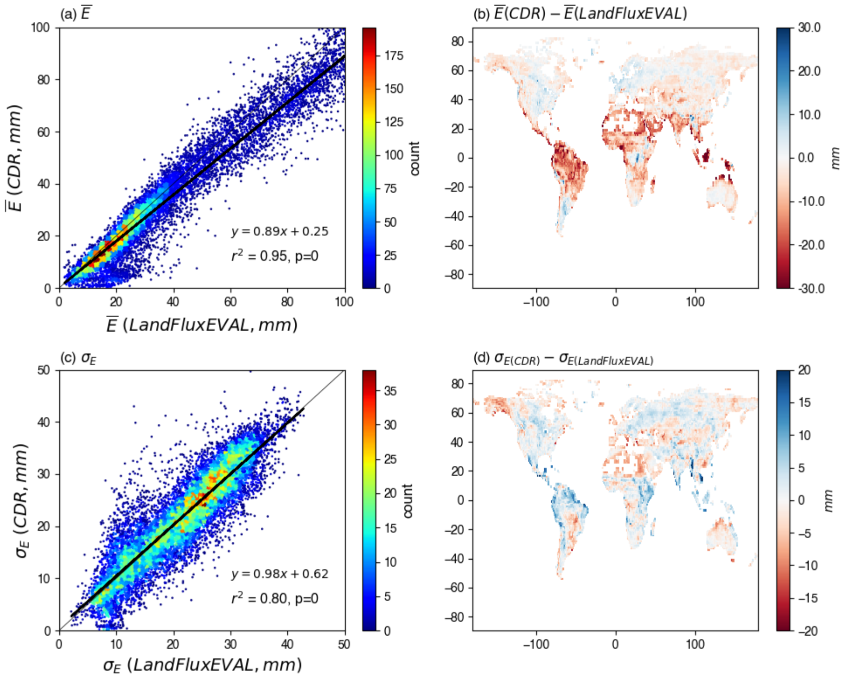

Figure S7. Comparison of monthly evapotranspiration E between LandFluxEVAL and Climate Data Record (CDR) databases. Top panels (a) (b) show comparison of the mean monthly ($\overline{E}$) while bottom panels (c) (d) show comparison of the standard deviation (σ_E) of monthly E.

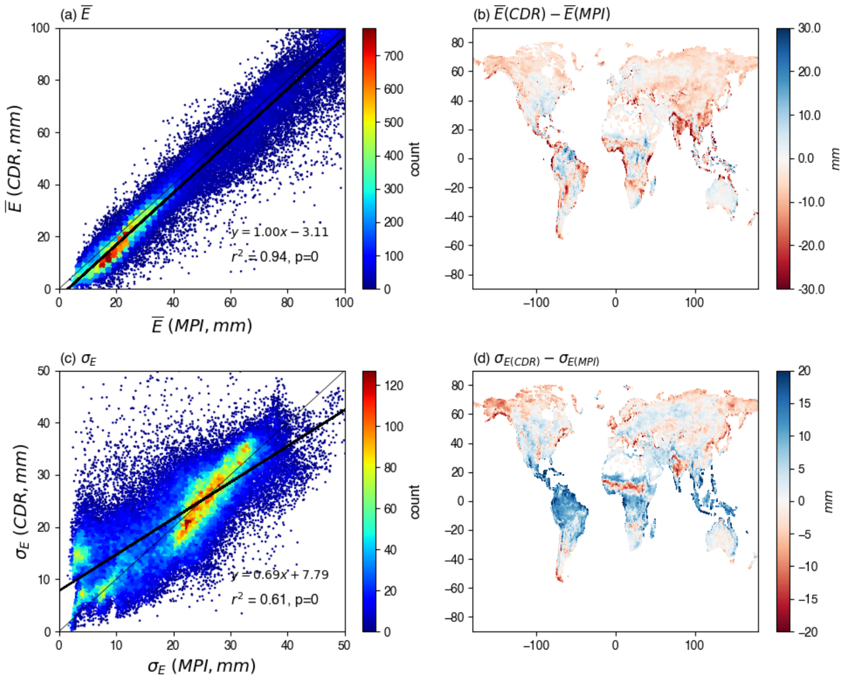

Figure S8. Comparison of monthly evapotranspiration *E* between Max Planck Institute (MPI) and Climate Data Record (CDR) databases. Top panels (a) (b) show comparison of the mean monthly ($\overline{E}$) while bottom panels (c) (d) show comparison of the standard deviation (σ_E) of monthly *E*.

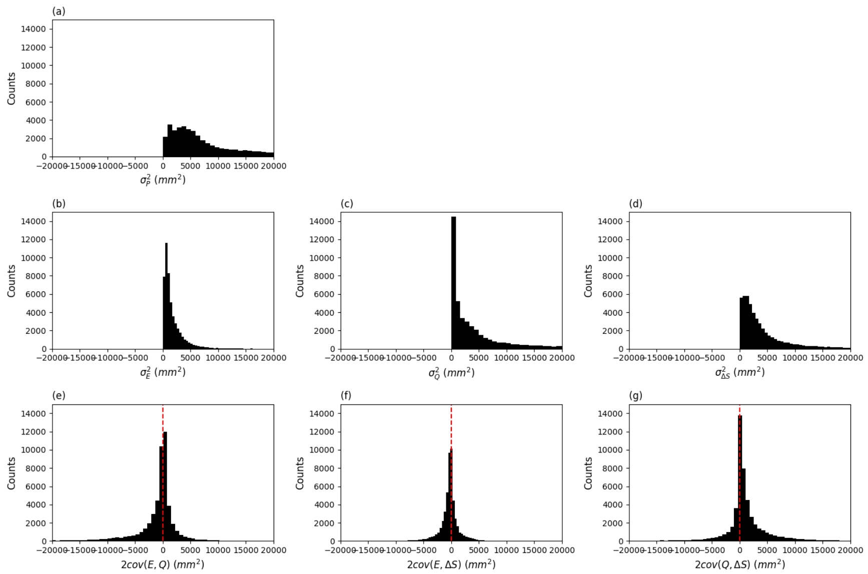

Figure S9. Distribution for each of the water cycle variances (σ_P^2, σ_E^2, σ_Q^2, $\sigma_{\Delta S}^2$) and covariances ($cov(E, Q)$, $cov(E, \Delta S)$, $cov(Q, \Delta S)$) shown in Fig. 3. Note that we have multiplied the covariances by two (see Eq. 2).

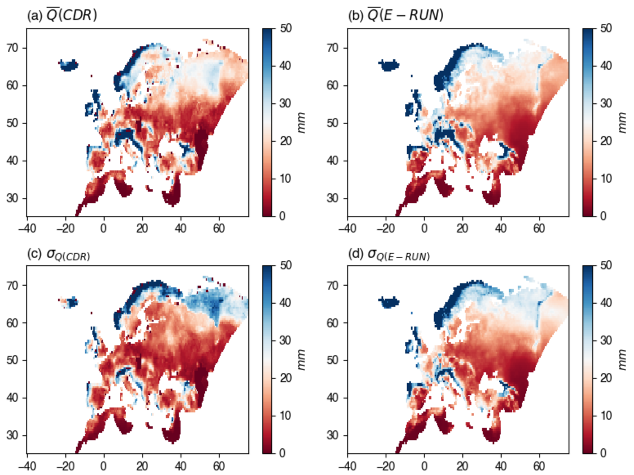

Figure S10. Mean ($\overline{Q}$) and standard deviation (σ_Q) of monthly runoff Q in the E-RUNOFF and Climate Data Record (CDR) databases in the area of spatial overlap (Europe). Top panels (a) (b) show the mean monthly ($\overline{Q}$) while bottom panels (c) (d) show the standard deviation (σ_Q) of monthly Q.

Formatted: Font:Times New Roman, Font color: Blue, Pattern: Clear (White)

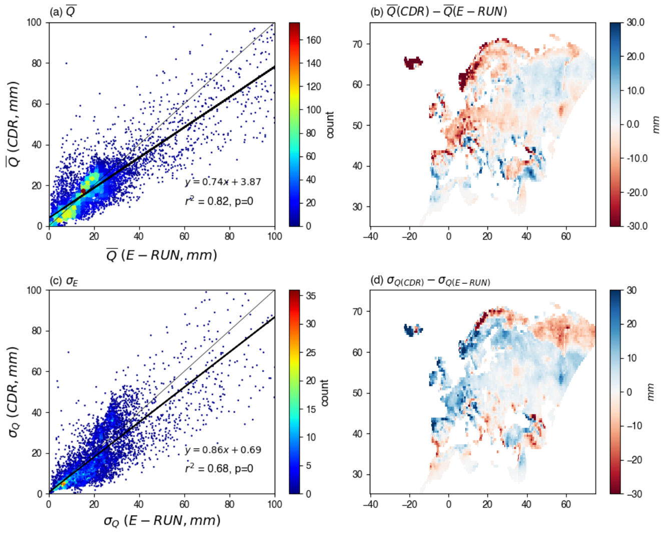

Figure S11. Comparison of monthly runoff Q between the E-RUNOFF and Climate Data Record (CDR) databases in the area of spatial overlap (Europe). Top panels (a) (b) show comparison of the mean monthly ($\overline{Q}$) while bottom panels (c) (d) show comparison of the standard deviation (σ_Q) of monthly Q.

Formatted: Font:Times New Roman, Font color: Blue, Pattern: Clear (White)

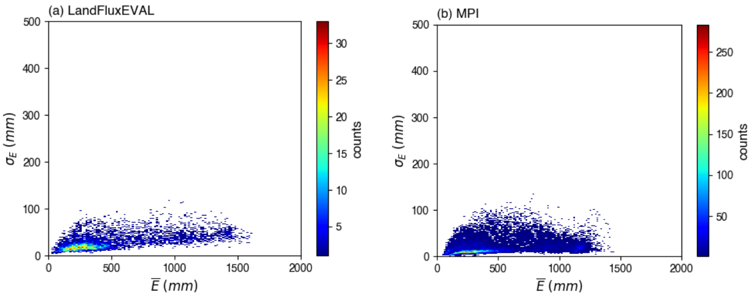

Figure S12. The same as Fig. 4b in main text but using evapotranspiration *E* data from the (a) LandFluxEVAL and (b) MPI databases.

Deleted: S10

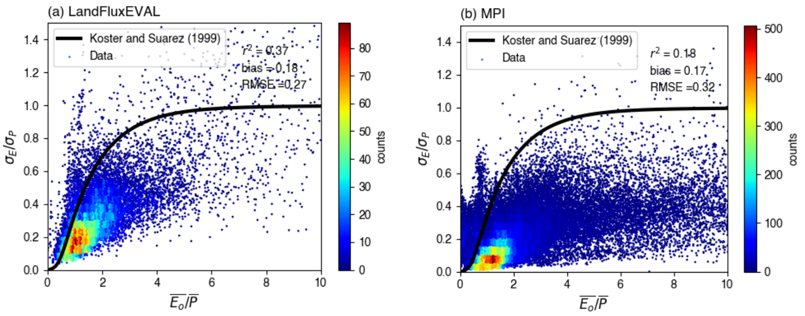

Figure S13. The same as Fig. 5a in main text but using evapotranspiration *E* data from the (a) LandFluxEVAL and (b) MPI databases.

Deleted: S11

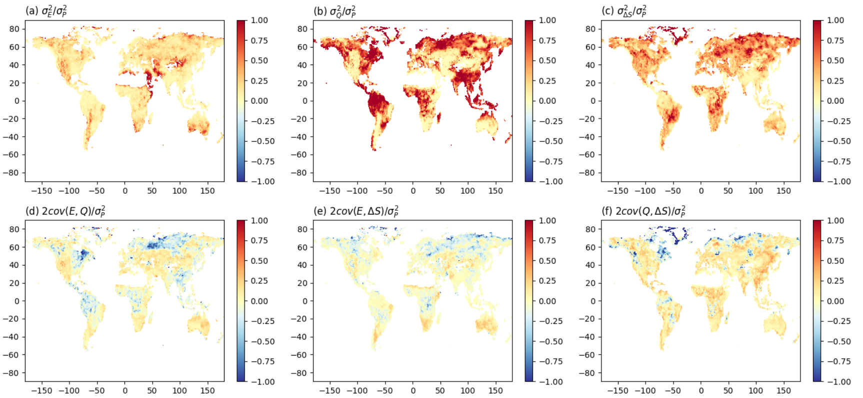

Figure S14. Inter-annual water cycle variances (σ_E^2, σ_Q^2, $\sigma_{\Delta S}^2$) and covariances ($cov(E,Q)$, $cov(E,\Delta S)$, $cov(Q,\Delta S)$) expressed as a fraction of the variance of P (σ_P^2). Note that we have multiplied the covariances by two (see Eq. 2).

Deleted: S12

Table S1. Summary of comparisons of monthly precipitation *P* and evapotranspiration *E* between observations at 32 FLUXNET sites and the CDR database.

Site ID	Site Name	Lat	Lon	Ref	Data period	r^2 (*P*)	bias (*P*, mm)	RMSE (*P*, mm)	r^2 (*E*)	bias (*E*, mm)	RMSE (*E*, mm)
AT_Neu	Neustift	47.1167	11.3175	Wohlfahrt et al., 2008	2004 - 2005, 2007 - 2010	**0.64**	53.54	61.53	**0.59**	-25.91	38.94
AU_Tum	Tumbarumba	-35.6566	148.1517	Leuning et al., 2005	2002 - 2010	**0.56**	1.08	39.34	**0.41**	-30.80	46.27
BE_Bra	Brasschaat	51.3076	4.5198	Carrara et al., 2004	1997 - 1998, 2000 -2002, 2007 - 2009	**0.64**	-3.05	26.66	**0.76**	14.70	20.55
CA_Qfo	Quebec - Eastern Boreal, Mature Black Spruce	49.6925	-74.3421	Bergeron et al., 2006	2005 - 2010	**0.57**	4.43	31.77	**0.85**	0.20	12.16
CH_Dav	Davos	46.8153	9.8559	Zielis et al., 2014	1997 - 2004, 2006 - 2010	**0.64**	82.53	91.39	**0.59**	-39.95	48.91
CH_Fru	Früebüel	47.1158	8.5378	Imer et al., 2013	2007 - 2010	**0.65**	-15.42	55.86	**0.63**	-15.97	33.05
DE_Geb	Gebesee	51.1001	10.9143	Anthoni et al., 2004	2001 - 2010	**0.69**	3.78	17.69	**0.78**	2.40	17.13
DE_Gri	Grillenburg	50.9500	13.5126	Prescher et al., 2010	2004 - 2010	**0.70**	-26.32	37.67	**0.90**	-8.10	15.99
DE_Hai	Hainich	51.0792	10.4530	Knohl et al., 2003	2000 - 2012	**0.70**	-10.35	23.17	**0.73**	6.31	20.26
DE_Kli	Klingenberg	50.8931	13.5224	Prescher et al., 2010	2006 - 2010	**0.68**	-13.61	28.05	**0.69**	-0.33	19.36
DE_Tha	Tharandt	50.9624	13.5652	Grünwald and Bernhofer, 2007	2000 - 2010	**0.66**	-18.71	32.35	**0.90**	-3.89	10.74
DK_Sor	Soroe	55.4859	11.6446	Pilegaard et al., 2011	2003 - 2010	**0.45**	-11.07	39.31	**0.69**	-8.45	25.35
FI_Hyy	Hyytiala	61.8474	24.2948	Suni et al., 2003	2006 - 2009	**0.78**	-7.07	20.43	**0.87**	-2.43	12.17
FR_Gri	Grignon	48.8442	1.9519	Loubet et al., 2011	2006 - 2010	**0.69**	-0.81	12.35	**0.72**	-19.15	27.07
FR_LBr	Le Bray	44.7171	-0.7693	Berbigier et al., 2001	1997 -1998, 2003 - 2008	**0.56**	-9.19	39.93	**0.49**	-7.65	28.08
IT_Cpz	Castelporziano	41.7053	12.3761	Garbulsky et al., 2008	2005 - 2007	**0.76**	-15.90	40.42	0.03	-9.23	31.69

IT_MBo	Monte Bondone	46.0147	11.0458	Marcolla et al., 2011	2003 - 2008	**0.36**	12.43	48.14	**0.88**	-14.78	21.92
NL_Loo	Loobos	52.1666	5.7436	Moors 2012	1999 - 2010	**0.56**	-2.16	24.78	**0.84**	-5.80	15.33
US_ARM	ARM Southern Great Plains site- Lamont	36.6058	-97.4888	Baldocchi and Sturtevant 2015	2003 - 2007	**0.71**	13.53	31.78	**0.61**	13.67	27.71
US_Los	Lost Creek	46.0827	-89.9792	Baker et al., 2003	2001 - 2003, 2005 - 2006	**0.52**	7.76	32.82	**0.87**	9.53	18.12
US_Me2	Metolius mature ponderosa pine	44.4523	-121.5574	Law (2002-2014)	2002 - 2005, 2007 - 2010	**0.54**	45.31	56.84	**0.82**	-12.91	19.36
US_MMS	Morgan Monroe State Forest	39.3232	-86.4131	Novick and Phillips (1999-2014)	2001 - 2010	**0.72**	6.60	31.44	**0.87**	-6.54	28.56
US_Ne1	Mead - irrigated continuous maize site	41.1651	-96.4766	Suyker (2001-2013a)	2002 - 2010	**0.45**	-6.64	51.86	**0.82**	-13.95	30.17
US_Ne2	Mead - irrigated maize-soybean rotation site	41.1649	-96.4701	Suyker (2001-2013b)	2002 - 2010	**0.56**	-8.77	46.45	**0.77**	-9.51	29.88
US_Ne3	Mead - rainfed maize-soybean rotation site	41.1797	-96.4397	Suyker (2001-2013c)	2004 - 2010	**0.88**	2.28	21.43	**0.78**	-2.92	24.61
US_NR1	Niwot Ridge Forest (LTER NWT1)	40.0329	-105.5464	Blanken (1998-2014)	2000 - 2010	**0.51**	-16.06	29.57	**0.84**	-28.44	30.58
US_SRM	Santa Rita Mesquite	31.8214	-110.8661	Barron-Gafford et al., 2011	2004 - 2010	**0.81**	1.34	15.40	**0.77**	-8.54	16.64
US_Syv	Sylvania Wilderness Area	46.2420	-89.3477	Desai et al., 2008	2002 - 2006	**0.33**	13.17	40.68	**0.90**	14.95	19.53
US_Ton	Tonzi Ranch	38.4316	-120.9660	Baldocchi et al., 2010	2002 - 2003, 2005 - 2009	**0.89**	14.68	27.44	**0.77**	-5.98	20.81

US_Var	Vaira Ranch- Ione	38.4133	-120.9507	Baldocchi et al., 2004	2001 - 2003, 2005 - 2010	**0.86**	16.91	30.92	**0.43**	3.77	25.84
US_Whs	Walnut Gulch Lucky Hills Shrub	31.7438	-110.0522	Biederman et al., 2016	2008 - 2010	**0.65**	1.89	21.26	**0.87**	-2.95	8.99
US_Wkg	Walnut Gulch Kendall Grasslands	31.7365	-109.9419	Biederman et al., 2016	2005 - 2010	**0.78**	1.59	15.66	**0.69**	-5.10	14.34

* Significant r^2 values (linear regression $p < 0.05$) are shown in bold.

References

Anthoni, P. M., and Coauthors, 2004: Forest and agricultural land-use-dependent CO2 exchange in Thuringia, Germany. *Global Change Biology*, **10,** 2005-2019.
B., L., and Coauthors, 2011: Carbon, nitrogen and Greenhouse gases budgets over a four years crop rotation in northern France. *Plant and Soil*, **343,** 109–137.
Baker, I., and Coauthors, 2003: Simulated And Observed Fluxes Of Sensible And Latent Heat And CO2 At The WLEF-TV Tower Using SiB2.5. *Global Change Biology*, **9,** 1262-1277.
Baldocchi, D., and C. Sturtevant, 2015: Does day and night sampling reduce spurious correlation between canopy photosynthesis and ecosystem respiration？. *Agricultural and Forest Meteorology*, **207,** 117-126.
Baldocchi, D. D., L. Xu, and N. Kiang, 2004: How plant functional-type, weather, seasonal drought, and soil physical properties alter water and energy fluxes of an oak–grass savanna and an annual grassland. *Agricultural and Forest Meteorology*, **123,** 13-39.
Baldocchi, D. D., and Coauthors, 2010: On the differential advantages of evergreenness and deciduousness in mediterranean oak woodlands: a flux perspective. *Ecological Applications*, **20,** 1583-1597.
Barron-Gafford, G. A., R. L. Scott, G. D. Jenerette, and T. E. Huxman, 2011: The relative controls of temperature, soil moisture, and plant functional group on soil CO2 efflux at diel, seasonal, and annual scales. *Journal of Geophysical Research: Biogeosciences*, **116**.
Berbigier, P., J. M. Bonnefond, and P. Mellmann, 2001: CO2 and water vapour fluxes for 2 years above Euroflux forest site. *Agricultural and Forest Meteorology*, **108,** 183-197.
Bergeron, O., H. A. Margolis, T. A. Black, C. Coursolle, A. L. Dunn, A. G. Barr, and S. C. Wofsy, 2006: Comparison of carbon dioxide fluxes over three boreal black spruce forests in Canada. *Global Change Biology*, **13,** 89-107.
Biederman, J. A., and Coauthors, 2016: Terrestrial carbon balance in a drier world: the effects of water availability in southwestern North America. *Global Change Biology*, **22,** 1867-1879.
Blanken, P., 1998-2014: FLUXNET2015 US-NR1 Niwot Ridge Forest (LTER NWT1).
Carrara, A., I. A. Janssens, J. Curiel Yuste, and R. Ceulemans, 2004: Seasonal changes in photosynthesis, respiration and NEE of a mixed temperate forest. *Agricultural and Forest Meteorology*, **126,** 15-31.
Desai, A. R., and Coauthors, 2008: Influence of vegetation and seasonal forcing on carbon dioxide fluxes across the Upper Midwest, USA: Implications for regional scaling. *Agricultural and Forest Meteorology*, **148,** 288-308.
Garbulsky, M. F., J. Penuelas, D. Papale, and I. Filella, 2008: Remote estimation of carbon dioxide uptake by a Mediterranean forest. *Global Change Biology*, **14,** 2860–2867.
Grünwald, T., and C. Bernhofer, 2007: A decade of carbon, water and energy flux measurements of an old spruce forest at the Anchor Station Tharandt. *Tellus B Chem. Phys. Meteorol.*, **59,** 387–396.
Imer, D., L. Merbold, W. Eugster, and N. Buchmann, 2013: Temporal and spatial variations of soil CO2, CH4 and N2O fluxes at three differently managed grasslands. *Biogeosciences*, **10,** 5931-5945.
Knohl, A., E. D. Schulze, O. Kolle, and N. Buchmann, 2003: Large carbon uptake by an unmanaged 250-year-old deciduous forest in Central Germany. *Agricultural and Forest Meteorology*, **118,** 151-167.
Law, B., 2002-2014: FLUXNET2015 US-Me2 Metolius mature ponderosa pine.
Leuning, R., H. A. Cleugh, S. J. Zegelin, and D. Hughes, 2005: Carbon and water fluxes over a temperate Eucalyptus forest and a tropical wet/dry savanna in Australia: measurements and comparison with MODIS remote sensing estimates. *Agricultural and Forest Meteorology*, **129,** 151-173.
Marcolla, B., and Coauthors, 2011: Climatic controls and ecosystem responses drive the inter-annual variability of the net ecosystem exchange of an alpine meadow. *Agricultural and Forest Meteorology*, **151,** 1233-1243.
Moors, E. J., 2012: Water Use of Forests in The Netherlands. PhD-thesis, Vrije Universiteit Amsterdam.
Novick, K., and R. Phillips, 1999-2014: FLUXNET2015 US-MMS Morgan Monroe State Forest.
Pilegaard, K., A. Ibrom, M. S. Courtney, P. Hummelshoj, and N. O. Jensen, 2011: Increasing net CO2 uptake by a Danish beech forest during the period from 1996 to 2009. *Agricultural and Forest Meteorology*, **151,** 934-946.
Prescher, A. K., T. Grunwald, and C. Bernhofer, 2010: Land use regulates carbon budgets in eastern Germany: From NEE to NBP. *Agricultural and Forest Meteorology*, **150,** 1016-1025.
Suni, T., and Coauthors, 2003: Long-term measurements of surface fluxes above a Scots pine forest in Hyytiälä, southern Finland, 1996–2001. *Boreal Environment Research*, **8,** 287-301.
Suyker, A., 2001-2013a: FLUXNET2015 US-Ne3 Mead - rainfed maize-soybean rotation site.
Suyker, A., 2001-2013b: FLUXNET2015 US-Ne2 Mead - irrigated maize-soybean rotation site.
Suyker, A., 2001-2013c: FLUXNET2015 US-Ne1 Mead - irrigated continuous maize site.

Wohlfahrt, G., A. Hammerle, A. Haslwanter, M. Bahn, U. Tappeiner, and A. Cernusca, 2008: Seasonal and inter-annual variability of the net ecosystem CO2 exchange of a temperate mountain grassland: effects of climate and management. *Journal of Geophysical Research: Atmospheres* **113,** D08110.
Zielis, S., S. Etzold, R. Zweifel, W. Eugster, M. Haeni, and N. Buchmann, 2014: NEP of a Swiss subalpine forest is significantly driven not only by current but also by previous year's weather. *Biogeosciences*, **11,** 1627-1635.